# Highly Efficient, Rapid, and Concurrent Removal of Toxic Heavy Metals by the Novel 2D Hybrid LDH-[Sn<sub>2</sub>S<sub>6</sub>]

Ahmet Celik<sup>a</sup>, David R. Baker, <sup>b</sup> Zikri Arslan, <sup>c</sup> Xianchun Zhu, <sup>d</sup> Alicia Blanton, <sup>a</sup> Jing Nie, <sup>a</sup> Shan Yang, <sup>a</sup> Shulan Ma, <sup>e</sup> Fengxiang X. Han, <sup>a</sup> Saiful M. Islam\*<sup>a</sup>

<sup>a</sup>Department of Chemistry, Physics, and Atmospheric Sciences, Jackson State University, Jackson, Mississippi, United States of America

<sup>b</sup>Sensors and Electron Devices Directorate, U. S. Army Research Laboratory, Adelphi, United States of America

<sup>c</sup>U.S. Geological Survey, MS 973, Federal Center, Denver, Colorado 80225, United States of America

<sup>d</sup>Department of Civil Engineering, Jackson State University, Jackson, Mississippi, United States of America

<sup>e</sup>College of Chemistry, Beijing Normal University, Beijing 100875, China

ABSTRACT: According to a United Nations' report, by 2050 nearly six billion people worldwide will suffer from clean water scarcity. This is mostly because of the exponential proliferation of world population, urbanization, industrialization, and water pollution. Heavy metals are common water pollutants that can pose grave public health consequences. Existing water purification systems lack materials that have the potential for quick, simultaneous, efficient, and cost-efficient removal of numerous toxic metals from wastewater. Here, we report the design and synthesis of an economically viable Layered Double Hydroxide - Stannic Sulfide, LDH–[Sn<sub>2</sub>S<sub>6</sub>] that exhibits a rapid, efficient, selective, and concurrent removal of Cu<sup>2+</sup>, Ag<sup>+</sup>, Cd<sup>2+</sup>, Pb<sup>2+</sup>, and Hg<sup>2+</sup> from ppm level to below 5 ppb satisfying World Health Organization's safe drinking water limit. Moreover, LDH–[Sn<sub>2</sub>S<sub>6</sub>] shows exceptionally high removal efficiencies of the above metals in acidic, neutral, and basic conditions. LDH–[Sn<sub>2</sub>S<sub>6</sub>] also demonstrates enormous sorption capacities of 378, 978,

332, 579, and 666 mg/g for Cu<sup>2+</sup>, Ag<sup>+</sup>, Cd<sup>2+</sup>, Pb<sup>2+</sup>, and Hg<sup>2+</sup>, respectively. Remarkably, LDH– [Sn<sub>2</sub>S<sub>6</sub>] displays extraordinary tolerance to the concentrations of Na<sup>+</sup>, Ca<sup>2+</sup>, Mg<sup>2+</sup>, Cl<sup>-</sup>, CO<sub>3</sub><sup>2-</sup>, NO<sub>3</sub><sup>-</sup>, SO<sub>4</sub><sup>2-</sup>, and other constituents in tap and river water; efficiently sequestrates Cu<sup>2+</sup>, Ag<sup>+</sup>, Cd<sup>2+</sup>, Pb<sup>2+</sup>, and Hg<sup>2+</sup> from parts per million (ppm) to safe drinking water levels in minutes. LDH–[Sn<sub>2</sub>S<sub>6</sub>] shows pseudo-second-order sorption kinetics suggesting chemisorption adsorption mechanism involving M-S bonding. Altogether, the regeneratable LDH–[Sn<sub>2</sub>S<sub>6</sub>] becomes an exceptional material that shows ultrahigh removal, unprecedented selectivity, rapid adsorption kinetics, wide pH stability, and a massive adsorption capacity. The integration of these features places LDH–[Sn<sub>2</sub>S<sub>6</sub>] at the top of all adsorbents known to date and thus could be used for wastewater purification.

### **Keywords:**

Heavy metals

Layered double hydroxides (LDHs)

Wastewater treatment

Metal sulfides intercalated LDH

Water purifications

#### 1. Introduction

Worldwide, currently more than one billion people lack access to clean and decontaminated drinking water. [1, 2] This leads to hundreds of millions of cases of water-related diseases and two to five million casualties each year. [3, 4] Among the different types of water contaminants, heavy metals pose severe concerns around the world because of their detrimental effects on humans and other biological systems.<sup>[5]</sup> The rapid surge of industrialization, urbanization, mining, fossil fuel burning as well as an exponential increase of the use of heavy metals has resulted in their accelerated accumulation in freshwater in recent decades. [2, 3, 6] Trace heavy metal cations such as mercury, lead, cadmium, silver, and copper commonly play a critical role in the contamination of water.<sup>[7]</sup> Decontamination of water from these heavy metal ions is essential because of their severe cytotoxicity to biological systems including human health. [8, 9] Therefore, over the past decades, an intensive effort has been devoted to the development of techniques and sorbent materials for the remediation of trace heavy metal cations from wastewater. [6, 10] Among the numerous techniques, physicochemical methods, coagulation and flocculation, electrochemical treatments, bio sorption, membrane filtration, adsorption, chemical precipitation, and ion-exchange are well known. [7,8,10,11] Despite improvements, efficient removal of heavy metals at trace levels is still the most challenging task. [7, 8, 11, 12] Chemical precipitation is the broadly applied method for heavy metals removal but the pH needs to be adjusted to perform chemical precipitation. [13, 14] Ionexchange can be used for high ion removal efficiency but most of the sorbents possess low selectivity for heavy metal ions.<sup>[10]</sup> Chemisorption and physisorption, on the other hand, are considered highly effective and economic methods because of their simple design, high sorption functionality, and low cost.<sup>[15]</sup> Numerous adsorbents such as zeolites,<sup>[16]</sup> activated carbon<sup>[17]</sup>, polymers,<sup>[18]</sup> biomaterials,<sup>[19]</sup> and sorption resins<sup>[20]</sup> have been used for the removal of metal ions,

but these materials often show poor selectivity, efficiency, stability, and sorption kinetics. Clays are also considered efficient natural adsorbents because of their low cost, high surface area, and hydrophilicity.<sup>[21]</sup> However, they suffer from poor affinity toward trace heavy metals, low selectivity and removal rates, sluggish sorption kinetics, and poor sorption capacity.

Sulfide-based materials show superior affinity toward heavy metal cations and can selectively bind Lewis acidic soft heavy metal ions following Pearson's hard-soft Lewis acid-base principles (HSAB). [10, 22-25] Thus, this class of materials has emerged as an efficient sorbent for soft heavy metal cations. [26-28] In recent years, different classes of metal sulfides including layered metal sulfides have been reported as superior sorbents for the removal of soft or relatively soft heavy metal cations. Some examples are: K2xMnxSn3-xS6 (KMS-1), [10, 27, 29, 30] H2xMnxSn3-xS6 (LHMS-1), [22, 31, 32] K2xMgxSn3-xS6 (KMS-2), [33, 34] K2xSn4-xS8-x (KTS-3), [35] open framework structures such as K6Sn[Zn4Sn4S17] [27] and [(Me)2NH2]2[GeSb2S6], [36] porous amorphous glass (A2A'2-x-SnSb2S6, A = Na; A' = K, Cs), [37] chalcogenide-based aerogels, [38] and metal sulfide-polypyrrole composites. [39, 40] These materials show selectivity toward heavy metals following the hard-soft Lewis acid-base paradigm. [24, 25]

Layered double hydroxides (LDHs) are a well-known type of anionic clay that consists of positively charged host layers and ion-exchangeable counter-anions in the interlayers. [41, 42] This class of clay possesses remarkable intercalation and anion-exchange properties. [43] These unique features of LDH stimulate us to intercalate them with soft Lewis basic sulfur species such as  $S_x^2$  (x = 2, 4) and  $MoS_4^2$  in the positively charged layers of MgAl–LDH and to study their sorption efficiencies of heavy metal cations. [41, 44, 45] Given LDHs' attractive 2D structural features, ion-exchange properties, flexibility in the accommodation of inter-layer anions, as well as the demand of ultra-high performing, cost-effective, scalable, high capacity adsorbents of heavy metal cations,

it is tremendously important to explore intercalation chemistry of LDHs with novel soft polarizable thioanions and study their adsorption features of heavy metals.

This study describes the intercalation of [Sn<sub>2</sub>S<sub>6</sub>]<sup>4-</sup> into the gallery of MgAl—LDH and investigates its effectiveness for the removal of heavy metal ions from aqueous solutions. The assynthesized hybrid functionalized lamellar MgAl—LDH—[Sn<sub>2</sub>S<sub>6</sub>] (LDH—[Sn<sub>2</sub>S<sub>6</sub>]) shows unprecedented removal efficiency of Zn<sup>2+</sup>, Cu<sup>2+</sup>, Ag<sup>+</sup>, Cd<sup>2+</sup>, Pb<sup>2+</sup> and Hg<sup>2+</sup> below the WHO limit for drinking water. Its extremely high sorption efficiencies, widespread selectivity, ultrafast sorption kinetics, wide range of pH stability, and reusability place this material at the top of hitherto known sorbents for heavy metals. Thus, this material becomes a promising sorbent for industrial-scale use for the decontamination of heavy metal polluted water.

#### 2. Materials and Methods

2.1 Synthesis: The MgAl—LDH—CO<sub>3</sub> was synthesized according to procedures described in previous work. [46] In detail, a mixture of 3.21 g Mg(NO<sub>3</sub>)<sub>2</sub>·6H<sub>2</sub>O (0.0125 mol), 2.34 g Al(NO<sub>3</sub>)<sub>3</sub>·9H<sub>2</sub>O (0.006 mol) and 2.28 g hexamethylenetetramine (HMT) were dissolved in 50 mL deionized water (DIW). Subsequently, the solution was hydrothermally treated at 140 °C for 24 h in a Teflon-autoclave. The as-prepared white precipitate of MgAl—CO<sub>3</sub>—LDH (LDH—CO<sub>3</sub>) was filtered, washed with DIW, and then dried under vacuum. MgAl—NO<sub>3</sub>—LDH (LDH—NO<sub>3</sub>) was synthesized by the exchange of CO<sub>3</sub><sup>2-</sup> by NO<sub>3</sub><sup>-</sup>, according to the literature. [46,47] Specifically, 127.5 g NaNO<sub>3</sub> and 0.36 mL HNO<sub>3</sub> (65%-68%) were dissolved in1000 mL of DIW and then 0.8 g of MgAl—LDH—CO<sub>3</sub> powder was added. The as-prepared mixture was sealed with Teflon and stirred for 24 h at room temperature. The resulting white solids were filtered, washed with DIW, and then vacuum-dried for 24 h. White crystals of Na<sub>4</sub>Sn<sub>2</sub>S<sub>6</sub>·14H<sub>2</sub>O were obtained from a solution

of 14.4 g Na<sub>2</sub>S·9H<sub>2</sub>O and 5.2 g SnCl<sub>4</sub>·5H<sub>2</sub>O in a refrigerator as previously described. Crystals of Na<sub>4</sub>Sn<sub>2</sub>S<sub>6</sub>·14H<sub>2</sub>O were filtered and washed with acetone and vacuum dried for 24 h. The  $[Sn_2S_6]^{4-}$  anions of the Na<sub>4</sub>Sn<sub>2</sub>S<sub>6</sub>·14H<sub>2</sub>O were exchanged with NO<sub>3</sub> of the LDH—NO<sub>3</sub> to synthesize the LDH– $[Sn_2S_6]$  in accordance with equation 1.

 $Mg_{0.66}Al_{0.34}(OH)_2(NO_3)_{0.34} \cdot 0.8H_2O + 0.085Na_4Sn_2S_6 \cdot 14H_2O \rightarrow$ 

$$Mg_{0.66}Al_{0.34}(OH)_2(Sn_2S_6)_{0.085} \cdot 0.8H_2O + 0.34NaNO_3$$
 (1)

For the synthesis of LDH—[Sn<sub>2</sub>S<sub>6</sub>], typically 0.25 g of LDH—NO<sub>3</sub> and 0.75 g of Na<sub>4</sub>Sn<sub>2</sub>S<sub>6</sub>·14H<sub>2</sub>O were dispersed in 50 mL DIW. The mixture was then stirred at ambient condition for 24 h leading to the formation of a yellowish solution of suspended particles. After filtration, yellow solids were obtained which were then washed with ethanol and dried at room temperature (RT) and pressure.

## 2.2 Heavy metal uptake experiments

The uptake (e.g., sorption) of heavy metal ions from aqueous solutions of various concentrations of Co<sup>2+</sup>, Ni<sup>2+</sup>, Cu<sup>2+</sup>, Zn<sup>2+</sup>, Ag<sup>+</sup>, Cd<sup>2+</sup>, Pb<sup>2+</sup>, and Hg<sup>2+</sup> were performed at ambient conditions. The sorption experiments were conducted using batch methods where the solid adsorbent, LDH–[Sn<sub>2</sub>S<sub>6</sub>], was mixed with the solutions of heavy metals for a certain time limit under vigorous stirring. After a certain period of interaction, the suspensions were centrifuged and the supernatant solutions were analyzed for the heavy metals using inductively coupled plasmamass spectrometry (ICP-MS). The adsorption efficiencies were calculated from the difference in the concentration of the metal cations before and after sorption.

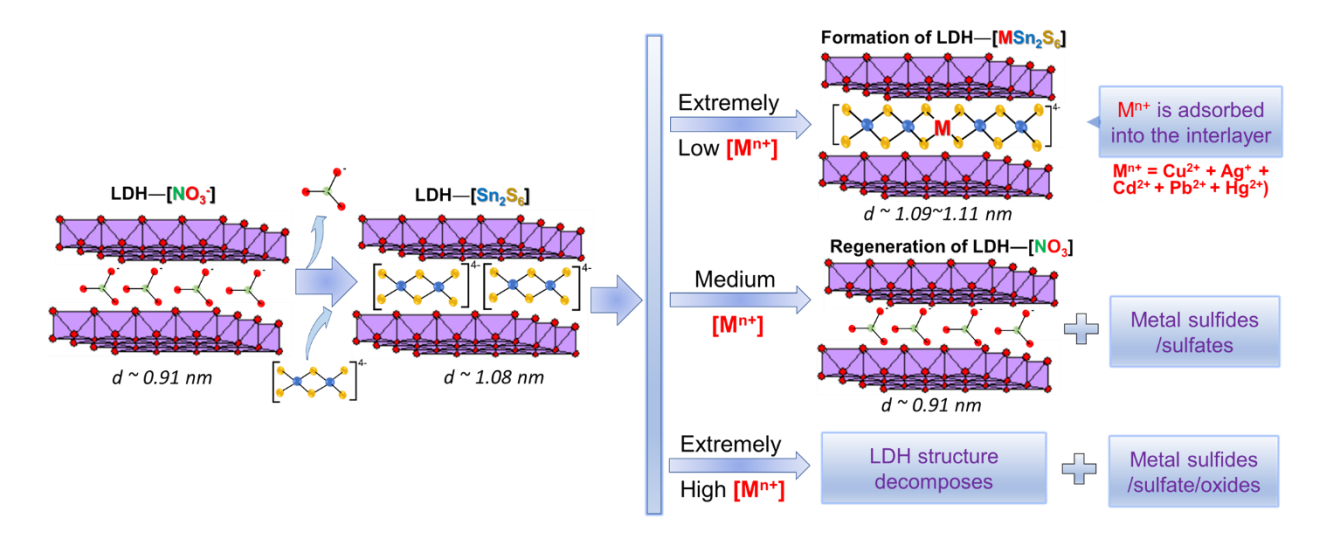
The distribution coefficient  $(K_d)$  in adsorption experiments was used to determine the affinity of LDH—Sn<sub>2</sub>S<sub>6</sub> for heavy metals. The  $K_d$  is defined by the equation:  $K_d = (V[(C_0 - C_f)/C_f])/(C_f)$  m; where V is the solution volume (mL),  $C_0$  and  $C_f$  correspond to the initial and the final

concentrations of the metal cations,  $M^{n+}$  ( $M^{n+}$  =  $Co^{2+}$ ,  $Ni^{2+}$ ,  $Cu^{2+}$ ,  $Zn^{2+}$ ,  $Ag^+$ ,  $Cd^{2+}$ ,  $Pb^{2+}$ , and  $Hg^{2+}$ ) in ppm (mg/L), and m is the mass of the solid sorbent (g).<sup>[29]</sup> The removal rate of  $M^{n+}$  was computed using the equation of  $100 \times (C_0 - C_f)/C_0$ . The removal capacity,  $q_m$  (mg/g) can be obtained from the equation:  $10^{-3} \times (C_0 - C_f)$  V/m. The adsorption experiments were carried out with V: m ratios of 1000 mL/g, at RT, and at different time scales ranging from min to several h.

#### 3. Results and discussion

# 3.1 Synthesis and Characterization of the LDH—[Sn<sub>2</sub>S<sub>6</sub>]

A new hybrid magnesium-aluminum layered double hydroxide, LDH–[ $Sn_2S_6$ ], was synthesized by the ion-exchange reaction of the  $NO_3^-$  anions in LDH— $NO_3$  with [ $Sn_2S_6$ ]<sup>4-</sup> anions and was investigated for its adsorption characteristics of  $Co^{2+}$ ,  $Ni^{2+}$ ,  $Cu^{2+}$ ,  $Zn^{2+}$ ,  $Ag^+$ ,  $Cd^{2+}$ ,  $Pb^{2+}$ , and  $Hg^{2+}$  as shown in Schematic 1.



**Schematic 1.** A schematic of the ion-exchange of NO<sub>3</sub><sup>-</sup> with Sn<sub>2</sub>S<sub>6</sub><sup>4-</sup> anions for the synthesis of LDH–[Sn<sub>2</sub>S<sub>6</sub>], the proposed concentration-dependent M<sup>n+</sup> adsorption phenomena leading to the adsorption of M<sup>n+</sup> into the interlayered gallery, and the regeneration of LDH—NO<sub>3</sub> with settlement of the neutral metal sulfides species outside the LDH gallery.

LDH-[Sn<sub>2</sub>S<sub>6</sub>] was synthesized at room temperature and pressure and is stable in air and water. To confirm the intercalation of [Sn<sub>2</sub>S<sub>6</sub>]<sup>4-</sup> anions into the gallery of MgAl-LDH the assynthesized material was characterized by energy dispersive X-ray spectroscopy (EDS), scanning electron microscopy (SEM), X-ray powder diffraction (XRD), Raman spectroscopy, X-ray photoelectron spectroscopy (XPS), and solid-state UV/Vis optical reflectance. Energy dispersive X-ray spectroscopy shows the presence of Sn and S in addition to Mg and Al in the LDH-Sn<sub>2</sub>S<sub>6</sub>. An average atomic abundance of Sn and S was determined at 5.17 and 15.90%, respectively, which is equivalent to a Sn:S ratio of 1.0:3.08. This value is close to that expected for Sn<sub>2</sub>S<sub>6</sub><sup>4-</sup>. Scanning electron microscopic (SEM) observations provide evidence of the retention of the plate like morphology even after the ion-exchange of the LDH—NO<sub>3</sub> with [Sn<sub>2</sub>S<sub>6</sub>]<sup>4-</sup> (Figure 1). This kind of retention of the morphology after the metal sulfides anion exchange was also observed for polysulfides, S<sub>x</sub> and MoS<sub>4</sub><sup>2-</sup> intercalated LDH.<sup>[44, 45]</sup> Elemental mapping shows the homogenous distribution of the Sn and S atoms throughout the hexagonal plates of LDH—[Sn<sub>2</sub>S<sub>6</sub>], further demonstrating consistent intercalation of [Sn<sub>2</sub>S<sub>6</sub>] anions (Figures 1D-G).

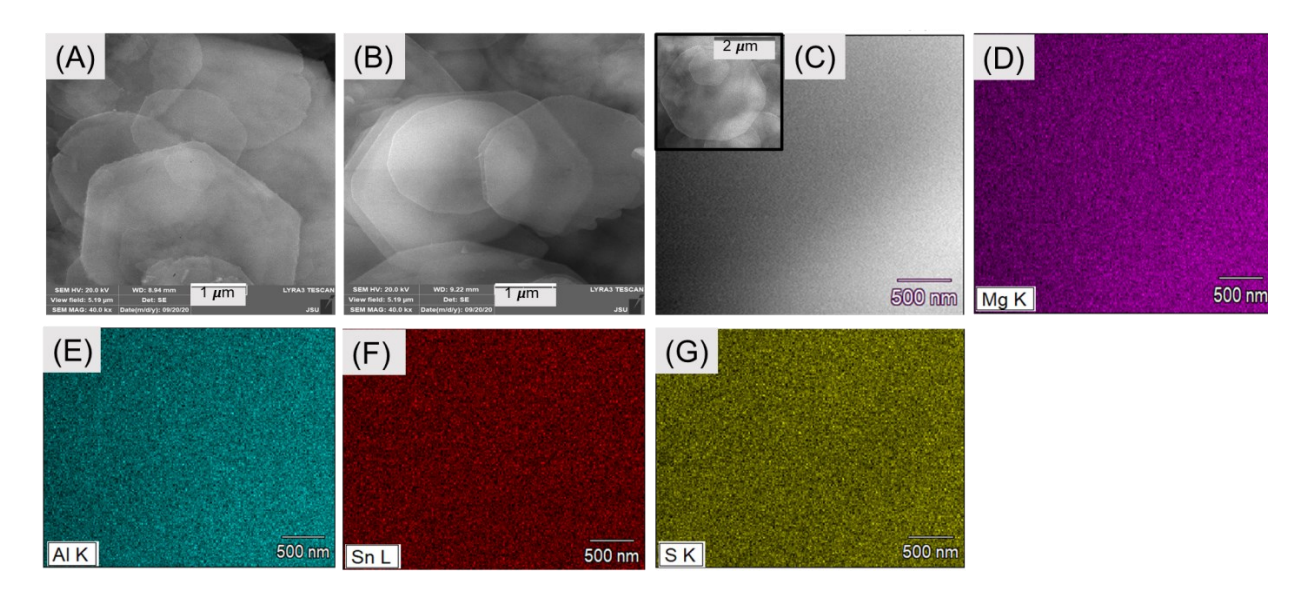


**Figure 1.** SEM images of the pristine LDH–NO<sub>3</sub> (A) and LDH–[Sn<sub>2</sub>S<sub>6</sub>] (B) showing well crystalline platelike morphology of the crystallites; section of the hexagonal crystals of LDH-Sn<sub>2</sub>S<sub>6</sub> (inset) (C) used for the elemental mapping of Mg, Al, Sn and S (D-G) showing the distributions of Mg, Al, Sn and S.

The evidence of the intercalation of [Sn<sub>2</sub>S<sub>6</sub>]<sup>4-</sup> into the layers of LDH was further investigated by XRD. A comparable feature of the XRD patterns of CO<sub>3</sub><sup>2-</sup>, NO<sub>3</sub><sup>-</sup>, and [Sn<sub>2</sub>S<sub>6</sub>]<sup>4-</sup> intercalated LDH is given in Figure 2A. The ion-exchange of CO<sub>3</sub><sup>2-</sup> by NO<sub>3</sub><sup>-</sup>, and subsequently by  $[Sn_2S_6]^{4-}$  led to a shift of the LDH's basal spacing ( $d_{basal}$ ) from 0.74 nm to 0.91 to 1.08 nm, respectively (Figure 2A). Such an increase in the basal spacing is due to the expansion of the unit cell parameter along the 00l crystallographic plane. Such an enlargement of the unit cell is in agreement with the intercalation of larger [Sn<sub>2</sub>S<sub>6</sub>]<sup>4-</sup> anions into the LDH. Intercalation of the [Sn<sub>2</sub>S<sub>6</sub>] into the LDH led to the color change of the samples from white (LDH–NO<sub>3</sub>) to yellow (LDH-[Sn<sub>2</sub>S<sub>6</sub>]). Solid-state optical absorption spectroscopy reveals that LDH-[Sn<sub>2</sub>S<sub>6</sub>] is a wide band gap semiconductor with an energy of ~3.0 eV (Figure S1, supporting information). The ionexchange of the nitrate by  $[Sn_2S_6]^{4-}$  was further confirmed by Raman spectroscopy. A comparable feature of the Raman spectra of Na<sub>4</sub>Sn<sub>2</sub>S<sub>6</sub>, LDH-[NO<sub>3</sub>], and LDH-[Sn<sub>2</sub>S<sub>6</sub>] is presented in Figure S2. For the pristine Na<sub>4</sub>Sn<sub>2</sub>S<sub>6</sub>, a series of vibrational bands were assigned at 163 cm<sup>-1</sup> (Na-S), 248 cm<sup>-1</sup> (Na-S), 355 cm<sup>-1</sup> (Sn-S) with the Sn-S band being the strongest. [49, 50] For LDH—[Sn<sub>2</sub>S<sub>6</sub>], a strong band centered at 325 cm<sup>-1</sup> is present while this peak is completely absent in the LDH—[NO<sub>3</sub>]. This further validates the incorporation of [Sn<sub>2</sub>S<sub>6</sub>] anions into the LDH. However, a slight shift of the bands can be attributed to the different chemical interactions of Sn<sub>2</sub>S<sub>6</sub> anions with positively charged LDH layers. The 1062 and 772 cm<sup>-1</sup> bands in LDH—NO<sub>3</sub><sup>[51, 52]</sup> are completely absent in the LDH-[Sn<sub>2</sub>S<sub>6</sub>] demonstrating the complete ion-exchange. In addition, bands at about 180 and 555 cm<sup>-1</sup> for the LDH—[NO<sub>3</sub>] and LDH—[Sn<sub>2</sub>S<sub>6</sub>] can be assigned as (M-

O) and (OH—M), respectively.<sup>[53]</sup> A small shift in the vibrational energy can be demonstrated as the chemical impact of the different anions.

XPS spectra of the LDH–[Sn<sub>2</sub>S<sub>6</sub>] revealed the existence of Sn and S with intense bands corresponding to binding energy (BEs) ranges of 157-163 and 482-495 eV, respectively (Figure 2B).<sup>[35,54,55]</sup> The bands at ~ 485.4 and 493.8 eV are consistent with the 3d<sub>3/2</sub> and 3d<sub>5/2</sub> energy levels of Sn<sup>4+</sup>.<sup>[35,55]</sup> The splitting of the 3d energy band of Sn<sup>4+</sup> is due to the presence of strong spin-orbital coupling.<sup>[55]</sup> In addition, the BE of the bands at 158.2, 159.5, 160.3, and 161.5 eV suggest the presence of S<sup>2+</sup> ions in the LDH–[Sn<sub>2</sub>S<sub>6</sub>]. However, the two sets of S<sup>2+</sup> peaks might be indicative of the different chemical interactions of S<sup>2+</sup> with the LDH layer hydroxides, probably by Sn—S···HO hydrogen bonding involving the hydroxide ions of the LDH layers.<sup>[35,54,56]</sup> The binding energies of the Sn 3d and S 2p show the presence of the Sn<sup>4+</sup> and S<sup>2-</sup> oxidation states of [Sn<sub>2</sub>S<sub>6</sub>]<sup>4+</sup> confirming its presence in the LDH structure. Photoelectron bands at 89.2 and 74.4 eV for LDH—NO<sub>3</sub> represent Mg 2s and Al 2p, respectively.<sup>[55]</sup> In contrast, LDH—Sn<sub>2</sub>S<sub>6</sub> displays Mg 2s and Al 2p at 86.6 and 73.4 eV, respectively. Such difference in the binding energies of the Mg 2s and Al 2p can be rationalized by the overall difference in the chemical environment of the NO<sub>3</sub><sup>-</sup> and Sn<sub>2</sub>S<sub>6</sub><sup>4+</sup> intercalated LDH.

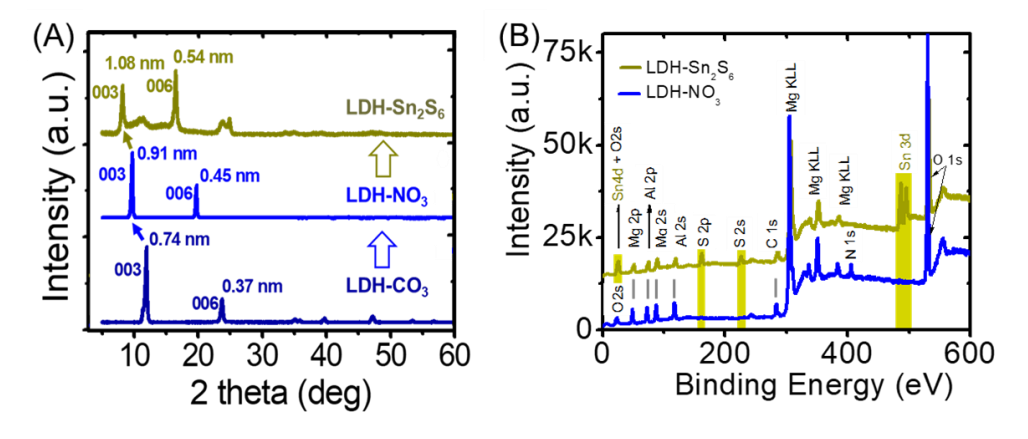


**Figure 2.** Comparable features of (A) XRD patterns of the LDH-CO<sub>3</sub>, LDH-NO<sub>3</sub> and LDH-Sn<sub>2</sub>S<sub>6</sub> showing the shift 003 and 006 peaks at lower Bragg angles with respect to the size of

the intercalated anions of  ${\rm CO_3}^{2^-}$ ,  ${\rm NO_3}^-$  and  ${\rm Sn_2S_6}^{4^-}$  and (B) XPS of the LDH-NO<sub>3</sub> and LDH-[Sn<sub>2</sub>S<sub>6</sub>] confirm the presence tin and sulfur in the LDH-[Sn<sub>2</sub>S<sub>6</sub>]. The XPS peaks were assigned based on the literature.<sup>[55,57]</sup>

# 3.2 Heavy Metal Removal by LDH-[Sn<sub>2</sub>S<sub>6</sub>]

The uptake study of the heavy metal ions ( $M^{n+} = \text{Co}^{2+}$ ,  $\text{Ni}^{2+}$ ,  $\text{Cu}^{2+}$ ,  $\text{Zn}^{2+}$ ,  $\text{Ag}^+$ ,  $\text{Cd}^{2+}$ ,  $\text{Pb}^{2+}$ , and  $\text{Hg}^{2+}$ ) was conducted using the batch method at ambient conditions. To determine the affinity of LDH–[ $\text{Sn}_2\text{S}_6$ ] toward the  $M^{n+}$  cations, 10 mg of sorbent material was suspended into the solutions of  $M^{n+}$  at different concentrations and pHs and interacted for different time intervals. The supernatant solutions were analyzed by ICP-MS to determine the remaining concentrations of  $M^{n+}$  after adsorption by LDH–[ $\text{Sn}_2\text{S}_6$ ].

At first, the adsorption experiments were conducted with individual solutions of the eight metal ions (Table 1) in DIW. As seen in Table 1, LDH–[Sn<sub>2</sub>S<sub>6</sub>] performed outstandingly for the sorption of Zn<sup>2+</sup>, Cu<sup>2+</sup>, Ag<sup>+</sup>, Cd<sup>2+</sup>, Pb<sup>2+</sup>, and Hg<sup>2+</sup> from aqueous solutions. The results showed that LDH—Sn<sub>2</sub>S<sub>6</sub> can adsorb over 99.9% of Cu<sup>2+</sup>, Ag<sup>+</sup>, Cd<sup>2+</sup>, Pb<sup>2+</sup>, and Hg<sup>2+</sup> from 10 ppm (mg/L) solutions of each cation. Such outstanding removal of Cu<sup>2+</sup>, Ag<sup>+</sup>, Cd<sup>2+</sup>, Pb<sup>2+</sup>, and Hg<sup>2+</sup> yielded final concentrations of ~ 4, 1, 1, 2, and 1 ppb, respectively. These metal ion concentrations are well below US EPA and WHO limits for drinking water.<sup>[58-59]</sup> Moreover, LDH–[Sn<sub>2</sub>S<sub>6</sub>] exhibits a distribution constant ( $K_d$ ) of ~10<sup>4</sup> mL/g for Zn<sup>2+</sup> and >10<sup>6</sup> mL/g for Cu<sup>2+</sup>, Ag<sup>+</sup>, Cd<sup>2+</sup>, Pb<sup>2+</sup>, and Hg<sup>2+</sup>. It is important to note that  $K_d$  represents the affinity of a sorbent toward a species and a value of  $\geq$ 10<sup>4</sup> mL/g is considered outstanding.<sup>[35, 53, 60]</sup> Hence, LDH–[Sn<sub>2</sub>S<sub>6</sub>] with such an excellent removal capacity, unprecedented selectivity toward a large number cations (Zn<sup>2+</sup>, Cu<sup>2+</sup>, Ag<sup>+</sup>, Cd<sup>2+</sup>, Pb<sup>2+</sup>, and Hg<sup>2+</sup>) and outstanding  $K_d$  place this material as the topmost candidate for the sorption of heavy metals from aqueous solutions.

**Table 1: Results from** adsorption studies of LDH– $[Sn_2S_6]$  with eight individual heavy metal cations (initial concentration: 10 ppm<sup>a,b</sup> in DIW).

Single ions	C <sub>i</sub> (ppm)	C <sub>f</sub> (ppm)	M <sup>n+</sup> removal %	$K_d$ (mL/g)
$\mathrm{Co}^{2+}$	10	9.5	5.00	$5.26 \times 10^{1}$
$Ni^{2+}$	10	9.4	6.00	$6.38 \times 10^{1}$
$Zn^{2+}$	10	0.62	93.80	$1.51 \times 10^{4}$
$Cu^{2+}$	10	0.004	99.96	$2.50 \times 10^{6}$
$egin{array}{l} { m Ag}^+ \ { m Cd}^{2+} \end{array}$	10	0.001	99.99	$1.0 \times 10^{7}$
$Cd^{2+}$	10	0.001	99.99	$1.0 \times 10^{7}$
$Pb^{2+}$	10	0.002	99.98	$5.0 \times 10^{6}$
$\mathrm{Hg}^{2+}$	10	0.001	99.99	$1.0 \times 10^{7}$

aion concentration: ~10 ppm per ion. Contact time: 3h;  ${}^bV$  =10 mL; mass of solid sample = 0.010 g; V/m ratio =1000 mL/g and pH~7.  $C_i$  = initial (pre-adsorption) concentration,  $C_f$  = final (post adsorption) concentration.

To determine the selective affinity and the competitive sorption of trace heavy metal cations, 10 mg of LDH– $[Sn_2S_6]$  sorbents were suspended into a solution that contained  $M^{n+} = Co^{2+}$ , Ni<sup>2+</sup>, Cu<sup>2+</sup>, Zn<sup>2+</sup>, Ag<sup>+</sup>, Cd<sup>2+</sup>, Pb<sup>2+</sup>, and Hg<sup>2+</sup> together, a solution that we call mixed-ion states (Table 2). A solution of 10 ppm for each of eight cations results in a total concentration of 80 ppm. The sorption experiment was conducted at pH ~7 for a contact time of 3h. Remarkably, even in the presence of mixed-competing ions, the affinity and the removal capacity of the sorbent was as high as for the individual cations Cu<sup>2+</sup>, Ag<sup>+</sup>, Cd<sup>2+</sup>, Pb<sup>2+</sup>, and Hg<sup>2+</sup> with the final concentrations of these cations as low as 5 ppb. More precisely, the removal capacity in the mixed-ion states is over 99.9% and  $K_d$  values reach ~10<sup>6</sup> mL/g for Cu<sup>2+</sup>, Ag<sup>+</sup>, Cd<sup>2+</sup>, Pb<sup>2+</sup> and Hg<sup>2+</sup>. At these concentrations, the selectivity order for these ions was Zn<sup>2+</sup>, Co<sup>2+</sup>, Ni<sup>2+</sup><< Ag<sup>+</sup>, Cu<sup>2+</sup>< Hg<sup>2+</sup>< Pb<sup>2+</sup>, Cd<sup>2+</sup>. The concurrent removal of such a large number of heavy metals ions ( Cu<sup>2+</sup>, Ag<sup>+</sup>, Cd<sup>2+</sup>, Pb<sup>2+</sup>, and Hg<sup>2+</sup>), excellent  $K_d$  values, and ultrahigh removal capacity for a single adsorbent is yet to be known in the literature. A comparison of the adsorption data for the individual and mixed cation experiments demonstrates that at neutral pH, LDH-Sn<sub>2</sub>S<sub>6</sub> is similarly effective in both systems for Cu<sup>2+</sup>, Ag<sup>+</sup>,  $Cd^{2+}$ ,  $Pb^{2+}$ , and  $Hg^{2+}$ . However, our results show the adsorption of  $Zn^{2+}$  dropped from ~ 94% ( $K_d$  $\sim 1.5 \times 10^4$ ) to  $\sim 6\%$  (5.5×10<sup>1</sup> mL/g) from the individual to mixed cations systems. This finding suggests that the  $Zn^{2+}$  cations are less selective for the LDH-Sn<sub>2</sub>S<sub>6</sub>. This could be due to its higher

chemical hardness and thus lower affinity for the chemically soft and polarizable sulfide anions. Overall, a combination of such outstanding sorption efficiencies establishes LDH–[Sn<sub>2</sub>S<sub>6</sub>] as a highly promising adsorbent for the removal of heavy metals from complex samples and wastewater treatment that we have discussed in more detail in section 4.

**Table 2.** Adsorption studies of LDH–[Sn<sub>2</sub>S<sub>6</sub>] toward mixed-eight ions with 10 ppm concentrations for each cations meaning 80 ppm all together in DIW.

Mixed-ions	C <sub>i</sub> (ppm)	C <sub>f</sub> (ppm)	M <sup>n+</sup> removal (%)	$K_d$ (mL/g)
$\mathrm{Co}^{2+}$	10	9.91	0.90	$0.91 \times 10^{2}$
$Ni^{2+}$	10	9.90	1.00	$1.01 \times 10^{1}$
$Zn^{2+}$	10	9.45	5.50	$5.82 \times 10^{1}$
$Cu^{2+}$	10	0.005	99.95	$2.00 \times 10^{6}$
$egin{array}{l} \operatorname{Ag}^+ \ \operatorname{Cd}^{2+} \end{array}$	10	0.005	99.95	$2.00 \times 10^{6}$
$Cd^{2+}$	10	0.001	99.99	$1.00 \times 10^7$
$Pb^{2+}$	10	0.001	99.99	$1.00 \times 10^7$
$\mathrm{Hg}^{2+}$	10	0.004	99.96	$2.50 \times 10^{6}$

contact time: 3h; V=10 mL; m (mass of solid sample) = 0.010g; V/m ratio = 1000 mL/g; and pH: 7.  $C_i$ = initial (pre-adsorption) concentration,  $C_f$ = final (post adsorption) concentration.

LDH–[Sn<sub>2</sub>S<sub>6</sub>] was also studied at pH ranging from 2 to 12 to determine the stability as well as the sorption efficiencies for Cu<sup>2+</sup>, Ag<sup>+</sup>, Cd<sup>2+</sup>, Pb<sup>2+</sup>, and Hg<sup>2+</sup> ions (Table S1). This experiment was conducted by 3 h interactions between cation solutions sorbents. Strikingly, our study revealed that LDH–[Sn<sub>2</sub>S<sub>6</sub>] could efficiently capture these cations within this pH range (Figure 3).

A detailed analysis of the pH dependent study shows that LDH-Sn<sub>2</sub>S<sub>6</sub> is the most efficient at adsorption of Cu<sup>2+</sup>, Ag<sup>+</sup>, Cd<sup>2+</sup>, Pb<sup>2+</sup>, and Hg<sup>2+</sup> ions at pH~7. At this pH, it achieves  $\geq$  99.9% removal of each cation with  $K_d$  values  $>10^6$  mL/g. At pH ~2,  $K_d$  values for Cu<sup>2+</sup>, Ag<sup>+</sup>, and Pb<sup>2+</sup> decrease about one order of magnitude and their removal rates decrease to 99.7, 99.5, and 99.0%, respectively. In contrast,  $K_d$  values remain  $>10^7$  mL/g for Hg<sup>2+</sup> in the pH range of 2 to 7. Remarkably, the  $K_d$  and removal rate for Cd<sup>2+</sup> remain at ~10<sup>6</sup> mL/g and >99.9%, respectively, over the pH range of ~2 to 12. At pH ~12, we observed similar results for the absorption of Cu<sup>2+</sup> and Ag<sup>+</sup> (~99.0%,  $K_d$ ~10<sup>5</sup> mL/g). On the contrary, the removal of Hg<sup>2+</sup> remains over 99.9 % in the pH

range of two to nine but decreases to  $\sim$ 72 % at pH  $\sim$ 12. The removal of Pb<sup>2+</sup> varies from 99% ( $K_d$   $\sim$ 10<sup>5</sup> mL/g) at pH  $\sim$ 2 to about 33% ( $K_d \sim$ 5.2×10<sup>2</sup> mL/g) at pH  $\sim$ 12. The decreased removal efficiencies of Pb<sup>2+</sup> and Hg<sup>2+</sup> at higher pH can be related to the gradual hydrolysis of the LDH. In contrast, the higher removal of Cu<sup>2+</sup>, Ag<sup>+</sup>, and Cd<sup>2+</sup> at pH  $\sim$ 12 could be a co-operative effect of both the adsorption and metal hydroxide precipitation. These high removal capacities and remarkably high distribution constants reveal LDH–[Sn<sub>2</sub>S<sub>6</sub>] as an unprecedented sorbent for the adsorption of heavy metals ions from acidic, alkaline, and neutral wastewater.

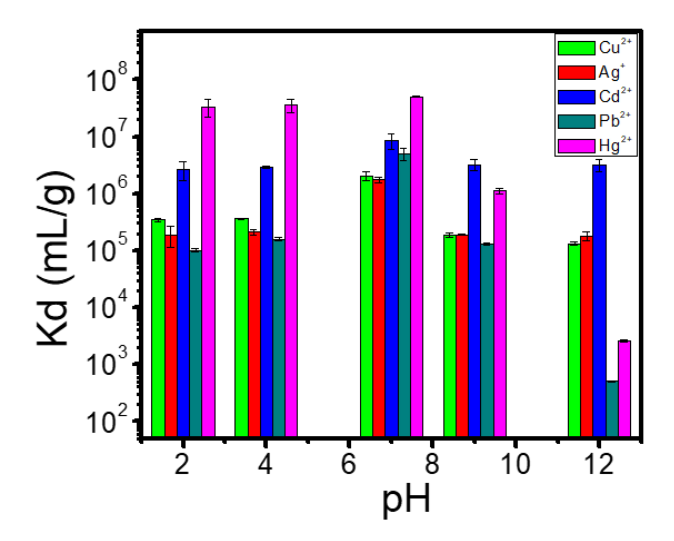


**Figure 3:** Distribution constants,  $K_d$  versus pH show the excellent sorption efficiencies of Cu<sup>2+</sup>,  $Ag^+$ ,  $Cd^{2+}$ ,  $Pb^{2+}$ , and  $Hg^{2+}$  in acidic, alkaline, and neutral media.

# 3.3 Adsorption Kinetic Studies of Cu<sup>2+</sup>, Ag<sup>+</sup>, Cd<sup>2+</sup>, Pb<sup>2+</sup>, and Hg<sup>2+</sup>

The kinetics for Cu<sup>2+</sup>, Ag<sup>+</sup>, Cd<sup>2+</sup>, Pb<sup>2+</sup>, and Hg<sup>2+</sup> adsorption by LDH–[Sn<sub>2</sub>S<sub>6</sub>] were studied to determine adsorption rates and understand the adsorption mechanism until it reaches equilibrium. In general, the adsorption rate is determined by two different rate equations, known as pseudo-first-order and pseudo-second-order mechanisms. Here, we used these mechanisms to analyze the adsorption phenomena of the LDH–[Sn<sub>2</sub>S<sub>6</sub>]. The comparison was then drawn between the experimental and calculated data. The two kinetic rate equations are as follows:<sup>[61]</sup>

Pseudo-first-order:

$$\ln(q_{\rm e} - q_{\rm t}) = \ln q_{\rm e} - k_1 t \tag{2}$$

Pseudo-second-order:

$$\frac{\mathrm{t}}{q_{\mathrm{t}}} = \frac{1}{k_2 q_{\mathrm{e}}^2} + \frac{\mathrm{t}}{q_{\mathrm{e}}} \tag{3}$$

Where,  $q_e$  (mg/g) is the amount of adsorbed element per unit mass of adsorbent at equilibrium and  $q_t$  (mg/g) is the adsorbed amount at time t, while  $k_1$  (min<sup>-1</sup>) and  $k_2$  (g/mg min<sup>-1</sup>) are rate constants of pseudo-first-order and pseudo-second-order adsorption interactions, respectively.<sup>[62]</sup> The  $k_1$  value was obtained by plotting  $\ln(q_e-q_t)$  against t and  $k_2$  by plotting  $t/q_t$  against t (Figure 4).

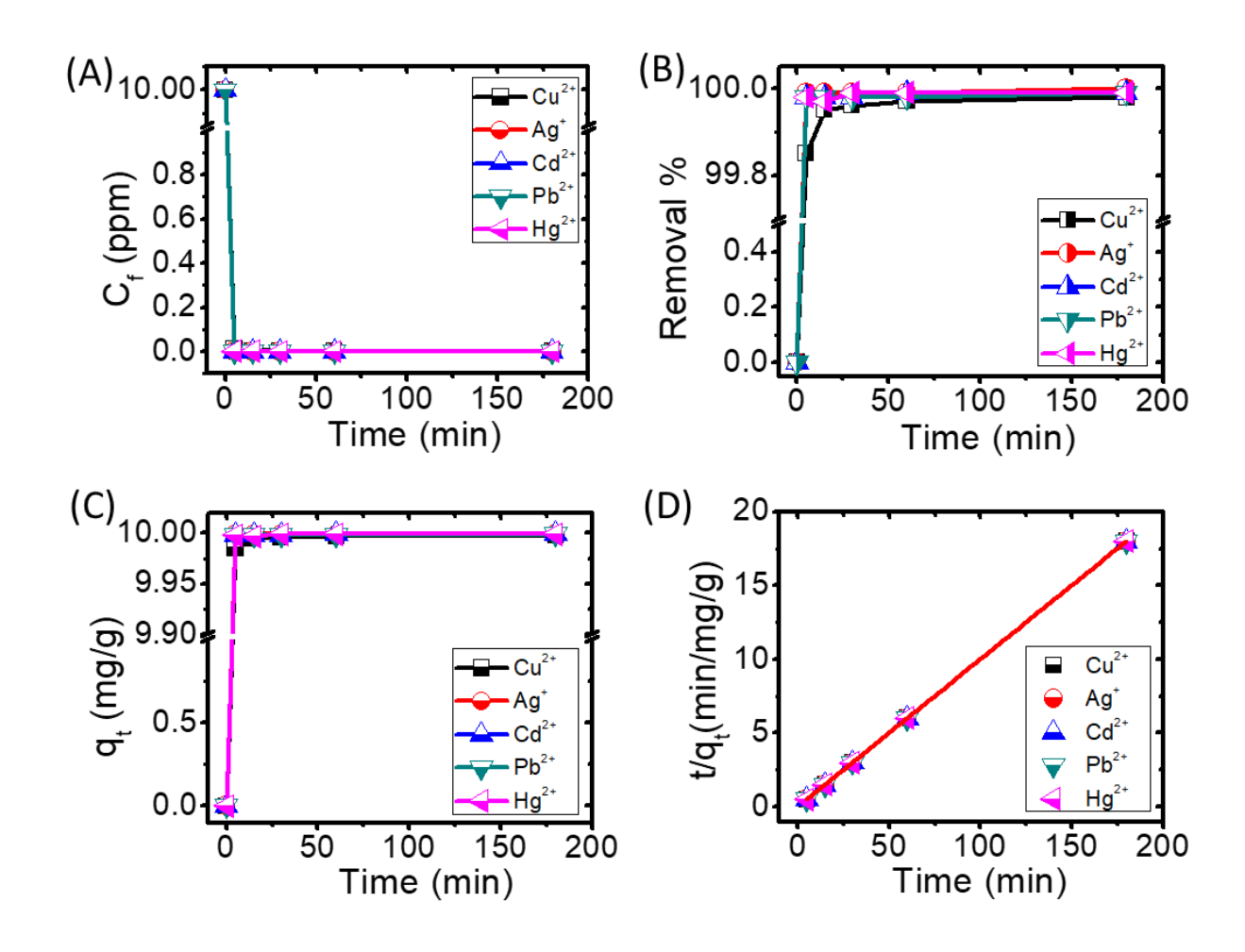


**Figure 4.** Adsorption kinetics curves for Cu<sup>2+</sup>, Ag<sup>+</sup>, Cd<sup>2+</sup>, Pb<sup>2+</sup>, and Hg<sup>2+</sup>; (A) Ion concentration change with contact time, (B) Removal % as a function of contact time, (C) Sorption capacity(q<sub>t</sub>) with contact time, and (D) pseudo-second-order kinetic plots.

As shown in Figure 4 and in Table S2, the adsorption rates for  $Cu^{2+}$ ,  $Ag^+$ ,  $Cd^{2+}$ ,  $Pb^{2+}$ , and  $Hg^{2+}$  ions in the DIW for 10 ppm of concentrations of each cation are extremely rapid. Within only 5 min, the LDH–[Sn<sub>2</sub>S<sub>6</sub>] achieved ~ 99.9 % removal of  $Cu^{2+}$ ,  $Ag^+$ ,  $Cd^{2+}$ ,  $Pb^{2+}$ , and  $Hg^{2+}$  with  $K_d$  values of over  $10^5$  mL/g for each cation. The removal capacity and  $K_d$  reached virtually ~100% and >10<sup>6</sup> mL/g, respectively, for all five cations within 1h. Overall, these experiments revealed that the adsorption for all five cations reaches equilibrium just in 5 min. A similar trend in the adsorption kinetics was observed for  $Hg^{2+}$  by LDH-MoS<sub>4</sub>, [45] and for  $Hg^{2+}$ ,  $Ag^+$ , and  $Pb^{2+}$  by polypyrrole-MoS<sub>4</sub>. [40] But to the best of our knowledge, such a rapid and efficient removal for a large number of cations,  $Cu^{2+}$ ,  $Ag^+$ ,  $Cd^{2+}$ ,  $Pb^{2+}$ , and  $Hg^{2+}$  down to trace levels by a single adsorbent has not been reported in the literature.

A plot of  $t/q_t$  against t showed a linear relationship for all five cations (Figure 4D). The kinetic parameters for  $Cu^{2+}$ ,  $Ag^+$ ,  $Cd^{2+}$ ,  $Pb^{2+}$ , and  $Hg^{2+}$  are summarized in Table S3. The calculated sorption capacities ( $q_{e,cal}$ ) derived from pseudo-second-order model are close to corresponding experimental values ( $q_{e,exp}$ ). The goodness of fit parameter ( $R^2$ ), is close to unity for all the cations. This indicates that adsorption for these ions onto LDH–[ $Sn_2S_6$ ] follows pseudo-second-order kinetics, suggesting that the adsorption follows chemisorption pathways. [63]

# 3.4 Adsorption isotherms and the uptake capacity for Cu<sup>2+</sup>, Ag<sup>+</sup>, Cd<sup>2+</sup>, Pb<sup>2+</sup>, and Hg<sup>2+</sup>

As shown in the above results, LDH–[ $Sn_2S_6$ ] exhibits high affinity to capture  $Cu^{2+}$ ,  $Ag^+$ ,  $Cd^{2+}$ ,  $Pb^{2+}$ , and  $Hg^{2+}$ . To determine the maximum sorption capacity of LDH–[ $Sn_2S_6$ ] for these

cations, an adsorption equilibrium study was carried out over a concentration ranging from 10 to 1500 ppm (Table S4). This study revealed increasing adsorption with the increasing concentrations of Cu<sup>2+</sup>, Ag<sup>+</sup>, Cd<sup>2+</sup>, Pb<sup>2+</sup>, and Hg<sup>2+</sup>(Figures 5 and S3) before reaching equilibrium.

LDH–[Sn<sub>2</sub>S<sub>6</sub>] achieved the maximum adsorption capacity of 378 mg/g for Cu<sup>2+</sup> (Figure S3, Table S4). With this high absorption capacity, LDH–[Sn<sub>2</sub>S<sub>6</sub>] outperforms the high performing adsorbents known to date.<sup>[44,45, 64-70]</sup> As an example, the adsorption capacity for Cu<sup>2+</sup> is much higher than highly performing sorbents, namely MoS<sub>4</sub>-LDH (181 mg/g),<sup>[45]</sup> PANI-PS (171 mg/g),<sup>[69]</sup>, KMS-1 (156 mg/g),<sup>[70]</sup> S<sub>x</sub>–LDH (127 mg/g),<sup>[44]</sup> and others (Table 3).

More strikingly, the LDH–[Sn<sub>2</sub>S<sub>6</sub>] exhibits ultra-high removal of Ag<sup>+</sup> over a wide range of initial concentrations (10 to 300 ppm). For the entire concentration range, the sorption of Ag<sup>+</sup> remains over 99.9% with  $K_d^{Ag}$  values of over 10<sup>5</sup> mL/g (Table S4). The maximum adsorption capacity (q<sub>m</sub><sup>Ag</sup>) reached a value of 978 mg/g (Figure S3, Table S4). As seen in Table 3, this value is exceptionally high when compared to other top materials such as Ni/Fe/Ti-MoS<sub>4</sub>-LDH (856 mg/g),<sup>[71]</sup> Mn-MoS<sub>4</sub> (564 mg/g),<sup>[72]</sup> MoS<sub>4</sub>-LDH (550 mg/g),<sup>[45]</sup> MoS<sub>4</sub>-ppy (480 mg/g at pH ~5),<sup>[40]</sup> and Mo<sub>3</sub>S<sub>13</sub>-Ppy (408 mg/g).<sup>[39]</sup>

Over 99% of Cd<sup>2+</sup>was removed for concentrations up to 50 ppm with  $K_d^{\text{Cd}}$  values in the range of ~10<sup>4</sup> to ~10<sup>6</sup> mL/g. The maximum adsorption capacity obtained was 332 mg/g, which is higher than any of the high performing Cd<sup>2+</sup> adsorbents listed Table 3 and comparable to KTS-3.<sup>[35]</sup> A similar removal rate (99.9%) was found for Pb<sup>2+</sup> for concentrations up to 50 ppm. The maximum capture capacity achieved for Pb<sup>2+</sup> (579 mg/g) was recorded for a 1500 ppm spiked solution. To the best of our knowledge this places LDH–[Sn<sub>2</sub>S<sub>6</sub>] at the top of all the high performing Pb<sup>2+</sup> adsorbents (Table 3).

We have also investigated the adsorption capacity of  $Hg^{2+}$  for a solution of 10 to 1500 ppm. Importantly, LDH–[Sn<sub>2</sub>S<sub>6</sub>] can remove  $\geq$  99.9% of  $Hg^{2+}$  from a 500 ppm solution (Table S4). At concentrations from 10 to 500 ppm, the  $K_d^{Hg}$  values remain in the range of  $10^5$ - $10^6$  mL/g. The maximum  $Hg^{2+}$  removal capacity of  $\sim$  666 mg/g is higher than any known adsorbents (Table 3). The outcome of this study suggests that LDH–[Sn<sub>2</sub>S<sub>6</sub>] is a unique adsorbent that outperforms for the sorption of a large number of heavy metals cations as discussed above (Table 3).

As seen in Table 3, metal sulfide or polysulfide intercalated LDHs, such as LDH-MoS4 and LDH- $S_x$  (x = 2-4) are highly efficient for the adsorption of heavy metal cations. [44,45] The novel LDH-Sn<sub>2</sub>S<sub>6</sub> is a new member of this family. As discussed above, the adsorption phenomena of heavy metals by the metal sulfides or polysulfides intercalated LDHs are mainly governed by the covalent interactions of the Lewis basic sulfide anions and the Lewis acidic soft heavy metal cations following the Hard-soft Lewis Acid-base paradigm<sup>[24, 25, 44, 45]</sup> Additionaly, this class of materials involves numerous Mn+ adsorption mechanisms, such as adduct formation in the interlayer spaces, metal-sulfide covalent interactions, and cation-exchange in the positively charged layers of the LDHs. Overall an integration of strong affinity of the sulfide species and numerous additional adsorption mechanisms makes metal sulfide or polysulfide intercalated LDHs superior adsorbents of heavy metals. Among the metal sulfide or polysulfide intercalated LDHs, LDH-Sn<sub>2</sub>S<sub>6</sub> exhibits the largest interlayer spacing that could facilitates the facile diffusion of cations into the interlayer spaces. However, the role of the host-guest interactions, relative interactions of M-S for MoS<sub>4</sub> and Sn<sub>2</sub>S<sub>6</sub> anions, and surface modifications for the adsorption of heavy metals by different metal sulfides/polysulfide intercalated LDHs cannot be ruled out. Overall, this study revealed that such tremendously higher adsorption capacities of such a large range of cations by a single adsorbent is not known to the best of our knowledge.

**Table 3.** Comparison of adsorption capacities for heavy metals with the known high performing sorbents

Cations	Adsorbents	q <sub>m</sub> (mg/g)	References and Journal name
Cu <sup>2+</sup>	$LDH-[Sn_2S_6]$	378	This work
	MoS <sub>4</sub> -LDH	181	<sup>[45]</sup> J. Am. Chem. Soc. <b>2016</b>
	PEI-modified biomass	92	<sup>[64]</sup> Environ. Sci. Technol. 2005
	TA-HTC	81	[65] Appl. Clay Sci. <b>2008</b>
	H100-LDH	85	[66] Chem. Eng. J.2015
	EDTA-LDH	71	[68] A.G. Anal. Material Process 2017
	Fe-MoS <sub>4</sub> Sx–LDH	117 127	[68] ACS Appl. Mater. Interfaces <b>2017</b> [44] J. Mat. Chem. <b>2014</b>
	PANI-PS	171	[69] ACS Appl. Mater. Interfaces 2015
	KMS-1	156	[70]J. Mol. Liq. <b>2014</b>
$\mathbf{Ag}^{^{+}}$	$LDH-[Sn_2S_6]$	978	This work
	Mo <sub>3</sub> S <sub>13</sub> -ppy	408	<sup>[39]</sup> J. Am. Chem. Soc. <b>2020</b>
	Ni/Fe/Ti–MoS4- LDH	856	<sup>[71]</sup> RSC Adv. <b>2020</b>
	$Mn-MoS_4$	564	<sup>[72]</sup> Chem. Eng. J. <b>2018</b>
	MoS <sub>4</sub> -Ppy	480 (pH $\approx$ 5) 725 (pH $\approx$ 1)	[40] Adv. Funct. Mater. <b>2018</b>
	MoS <sub>4</sub> -LDH	450	<sup>[45]</sup> J. Am. Chem. Soc. <b>2016</b>
	Sx-LDH	383	<sup>[44]</sup> J. Mat. Chem. A <b>2014</b>
	KMS-2	408	[33]Chem. Mater. 2015
	Fe-MoS <sub>4</sub>	565	[68]ACS Appl. Mater. Interfaces2017
$Cd^{2+}$	$LDH-[Sn_2S_6]$	332	This work
	DPA-LDH	258	[73]Chem. Eng. J. <b>2017</b>
	Biomass based hydrogel	161	<sup>[74]</sup> Sci. Rep, <b>2020</b>
	NH <sub>2</sub> -Functionalized	177	<sup>[75]</sup> Ind. Eng. Chem. Res. <b>2017</b>
	Zr-MOFs		
	Polysulfide-LDH	57	<sup>[44]</sup> J. Mat. Chem. <b>2014</b>
Pb <sup>2+</sup>	$LDH-[Sn_2S_6]$	579	This work
	MOF/polydopamine	394	<sup>[76]</sup> ACS Cent. Sci. <b>2018</b>
	MoS <sub>4</sub> -LDH	290	[45] J. Am. Chem. Soc. <b>2016</b>
	Mn-MoS <sub>4</sub>	357	<sup>[72]</sup> Chem. Eng J. <b>2018</b>
	Fe-MoS <sub>4</sub>	345	<sup>[68]</sup> ACS Appl. Mater. Interfaces <b>2017</b>
	EDTA-LDH	180	<sup>[77]</sup> Chem. Lett. <b>2004</b>

	Cellulose based	240	<sup>[78]</sup> ACS Appl. Mater. Interfaces <b>2015</b>
	charcogel Biomass based hydrogel	422.7	<sup>[74]</sup> Sci. Rep. <b>2020</b>
Hg <sup>2+</sup>	$LDH-[Sn_2S_6]$	666	This work
J	$MoS_4$ -LDH	500	<sup>[45]</sup> J. Am. Chem. Soc. <b>2016</b>
	Mn- MoS <sub>4</sub>	594	<sup>[72]</sup> Chem. Eng. J. <b>2018</b>
	Fe-MoS <sub>4</sub>	582	<sup>[68]</sup> ACS Appl. Mater. Interfaces <b>2017</b>
	MOF/PDA	1634	<sup>[76]</sup> ACS Cent. Sci. <b>2018</b>
	KMS-2	297	<sup>[33]</sup> Chem. Mater. <b>2015</b>
	MoS <sub>4</sub> -Ppy	210	<sup>[39]</sup> Adv. Funct. Mater. <b>2018</b>
	KMS-1	377	[32] Adv. Funct. Mater. <b>2009</b>

We used the Langmuir isotherm to model experimentally obtained adsorption data. This model predicts that adsorbate moieties undergo monolayer type coverage on the surface of the adsorbent. It assumes that once an adsorption site is occupied, no further adsorption can occur at the same site. The Langmuir isotherm model is shown as equation (4):

$$q = q_m \frac{bCe}{1 + bCe} \tag{4}$$

where  $C_e$  (mg/L) is the concentration at equilibrium, q (mg/g) is the equilibrium sorption capacity of the adsorbed M<sup>n+</sup> (Cu<sup>2+</sup>, Ag<sup>+</sup>, Cd<sup>2+</sup>, Pb<sup>2+</sup>, and Hg<sup>2+</sup>),  $q_m$  (mg/g) is the theoretical maximum sorption capacity, b (L·mg<sup>-1</sup>) is the Langmuir constant, and  $C_e$  (mg/L) is the equilibrium concentration. The equilibrium adsorption isotherms for Cd<sup>2+</sup>, Pb<sup>2+</sup>, and Hg<sup>2+</sup> are shown in Figure 5. The experimentally obtained data for the adsorption of each cation are fitted with the Langmuir model. The correlation coefficient, R<sup>2</sup> was  $\geq$  0.98 for Cu<sup>2+</sup>, 0.93 for Ag<sup>+</sup>, 0.98 for Hg<sup>2+</sup>, 0.95 for Cd<sup>2+</sup>, and 0.98 for Pb<sup>2+</sup> suggesting a good fit with the Langmuir model (Figures 5 and S3).

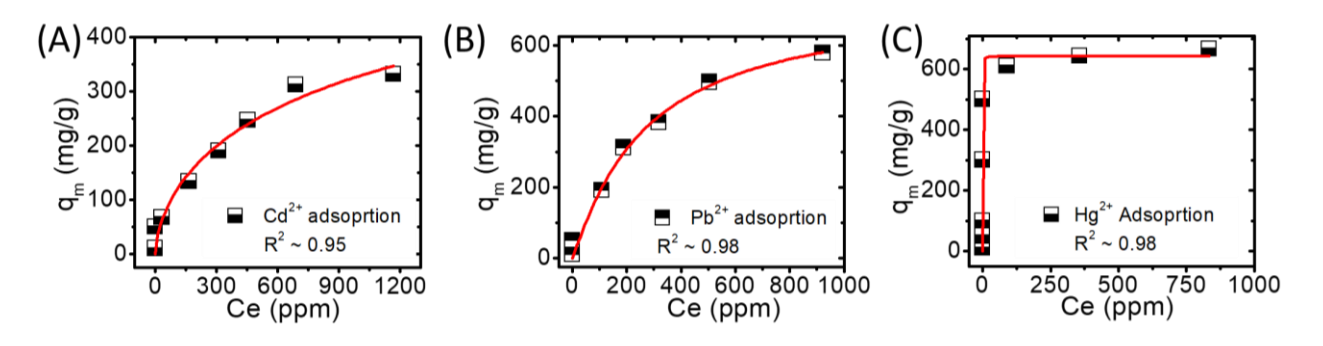


**Figure 5:** Sorption isotherms of Cd<sup>2+</sup> (A), Pb<sup>2+</sup> (B), and Hg<sup>2+</sup> (C) at pH~7, derived from the experimental data fitted with Langmuir model at equilibrium concentrations (Ce) and adsorption capacity (q<sub>m</sub>).

Considering the anion, [Sn<sub>2</sub>S<sub>6</sub>]<sup>4</sup> as the adsorption site for the capture of heavy metal ions, one can determine the theoretical maximum adsorption capacity based on the content of [Sn<sub>2</sub>S<sub>6</sub>]<sup>4</sup>in the LDH. The molecular weight of LDH-[Sn<sub>2</sub>S<sub>6</sub>] is 110 g based on its chemical formula  $Mg_{0.66}Al_{0.34}(OH)_2(Sn_2S_6)_{0.085} \cdot 0.8H_2O$  with a contribution from the  $Sn_2S_6$  moiety of 36.53 g/mol. Therefore, 1 g of LDH-[ $Sn_2S_6$ ] contains  $7.7 \times 10^{-4}$  mol (1 g× 0.085 mol / 110 g) of [ $Sn_2S_6$ ]<sup>4</sup>. In parallel to LDH-MoS<sub>4</sub>, [45] the adsorption mechanisms for LDH-[Sn<sub>2</sub>S<sub>6</sub>] is assumed as the binding of M<sup>n+</sup> cations with [Sn<sub>2</sub>S<sub>6</sub>]<sup>4-</sup> toward the formation of an adduct. Consequently, in the case of Ag<sup>+</sup> sorption, one mol of  $[Sn_2S_6]^{4-}$  will bind with maximum 4 mol of  $Ag^+$  to yield a theoretical maximum sorption capacity of Ag<sup>+</sup> is 333 mg (= $7.7 \times 10^{-4}$  mol  $\times 4 \times 108$  g/mol  $\times 10^{3}$  mg). Similarly, the theoretical maximum adsorption capacity for the divalent cations (2M<sup>2+</sup>:[Sn<sub>2</sub>S<sub>6</sub>]<sup>4-</sup>) is 98 mg for Cu<sup>2+</sup>, 173 mg for Cd<sup>2+</sup>, 308 mg for Hg<sup>2+</sup>, and 319 mg for Pb<sup>2+</sup>. In contrast, the maximum experimental sorption capacities were obtained as 378 mg for Cu<sup>2+</sup>, 978 mg for Ag<sup>+</sup>, 332 mg for Cd<sup>2+</sup>, 579 mg for Pb<sup>2+</sup>, and 666 mg for Hg<sup>2+</sup> (Tables 3 and S4). Here, the experimental adsorption capacity for each cation is substantially larger than the value determined based-on the abovementioned binding mechanism of charge balance. This suggests that the adsorption mechanism is more complex, and may involve different or multiple mechanisms.

At this stage, we consider each sulfide (S<sup>-2</sup>) of the  $[Sn_2S_6]^{4-}$  as an active site for covalent bonding interactions with M<sup>n+</sup> to form M-S chemical boding. There are 4.6×10<sup>-3</sup> moles of S in 1 g of  $Mg_{0.66}Al_{0.34}(OH)_2(Sn_2S_6)_{0.085} \cdot 0.8H_2O$ . Based on M–S covalent bonding,  $M^{2+}$ :  $S^{2-}=1:1$  ( $M^{2+}=1:1$ ) ( $M^{2+}=1:$  $Cu^{2+}$ ,  $Cd^{2+}$ ,  $Pb^{2+}$  and  $Hg^{2+}$ ) and  $M^+$ :  $S^{2-}=2:1$  ( $M^+=Ag^+$ ), one can determine the theoretical saturation limit for the adsorption capacity. Therefore, the theoretical maximum sorption capacity of Ag<sup>+</sup> for the covalent bonding mechanism is 994 mg/g (=  $4.6 \times 10^{-3}$  mol  $\times$  2  $\times$  108 g/mol  $\times 10^{3}$ mg). Similarly, the maximum theoretical adsorption capacity for Cu<sup>2+</sup>, Cd<sup>2+</sup>, Pb<sup>2+</sup>, and Hg<sup>2+</sup> is 292, 517, 952, and 920 mg/g, respectively. The similarity between the covalent bonding theoretical sorption capacity for Ag<sup>+</sup> (994 mg/g) and the experimental capacity (978 mg/g) suggests the validity of this mechanism. The formation of Ag<sub>2</sub>S and AgSO<sub>4</sub> in the final products of the adsorbed samples further validates this binding mechanism. For Cu<sup>2+</sup>, the experimental adsorption capability of 378 mg/g surpasses the theoretical capacity of 292 mg/g. This additional adsorption could be attributed to the incorporation of Cu<sup>2+</sup> in the Mg/Al octahedral sites of the LDH layers by substitution. Hence, higher concentration of Cu<sup>2+</sup> may facilitate the substitution of Cu<sup>2+</sup> by Mg<sup>2+</sup>. This kind of phenomenon was reported for  $K_{2x}Mg_xSn_{3-x}S_6$  (x = 0.5-1).[33, 34] On the other hand, experimental adsorption capacities for Cd<sup>2+</sup>, Hg<sup>2+</sup>, and Pb<sup>2+</sup> satisfy none of the mechanisms alone. Since the experimental sorption capacities remain somewhere in between mechanism M<sup>n+</sup>/[Sn<sub>2</sub>S<sub>6</sub>]<sup>4-</sup> adducts formation and M<sup>n+</sup>–S<sup>2-</sup> covalent bonding, one can assume a combination of the mechanisms. The possibility of the partial substitution of layered Mg<sup>2+</sup> by M<sup>n+</sup>, especially by Cd<sup>2+</sup> as we discussed above for Cu<sup>2+</sup>cations, cannot be ruled out. Overall, the different adsorption phenomena of the 2D Hybrid LDH-[Sn<sub>2</sub>S<sub>6</sub>] for heavy metals can be demonstrated by hard-soft Lewis acid base (HSAB) principle. [24, 25] In accordance with this principle, chemically soft and polarizable Lewis basic sulfide anions will prefentially bind with soft Lewis acidic heavy metal

cations. Hence, the degree of the M-S bonding interactions depends on the relative chemical hardness of cations. Apart from this, the adsorption of transition metals, such as  $Cu^{2+}$  and  $Cd^{2+}$ , especially at higher concentrations, can be achieved by the exchange with  $Mg^{2+}$  cations of the positively charged layer of  $[Mg_xAl_{1-x}O_6]$  octahedra. Here the cation-exchange could be facilitated by the relatively preferred coordination preferences to the octahedral geometry of the  $[Mg_xAl_{1-x}O_6]$  (e.g., oxides) layer of LHD.

### 3.5 Morphology and structural characterization of post-adsorption solid samples

To understand the structure, morphology, and physicochemical interactions of the sorbents toward the heavy metal cations, the solid sorbents were collected after the sorption experiments, dried, and analyzed by SEM-EDS, XRD, and XPS.

SEM images show that retention of the platelike hexagonal morphology of the LDH– [Sn<sub>2</sub>S<sub>6</sub>] crystallites is related to the concentrations of the M<sup>n+</sup>. For example, after treating the samples at concentrations of 10 and 100 ppm, the adsorbates seem to maintain the platelike morphology (Figure 6) indicating that the layered structure still dominates after cation sorption. A similar phenomenon was also observed in other intercalated LDH during adsorption of heavy metal cations. [41, 44, 45] In contrast, at extremely high concentrations of M<sup>n+</sup>, here in the case of 1500 ppm, the platelike morphology of the LDH-Sn<sub>2</sub>S<sub>6</sub> is absent. Instead, we can see the formation of aggregated nanoparticles. EDS analyses of LDH-Sn<sub>2</sub>S<sub>6</sub> treated with M<sup>n+</sup> show that the quantity of the metal cation increases with the increase of the initial concentrations of the respective metal ions (Table S5-9). This finding is in agreement with the increased adsorption of M<sup>n+</sup> cations with the higher initial concentrations as discussed above.

The adsorption of  $M^{n^+}$  was achieved at different concentrations in the range of 100 ppb to 1500 ppm. At extremely low concentration (~100 ppb) the basal space of post-adsorbed LDH–[Sn<sub>2</sub>S<sub>6</sub>]

expands from 1.08 to 1.10 nm for Pb<sup>2+</sup> and Cd<sup>2+</sup> and to 1.09 nm for Ag<sup>+</sup>, Cu<sup>2+</sup> and Hg<sup>2+</sup>. This suggests that, at such an extremely low concentration, the interlayer  $Sn_2S_6^{4+}$  anions holds the M<sup>n+</sup> cations and the structure of LDH–[ $Sn_2S_6$ ] dominates. A similar observation was reported for the polysulfide and  $MoS_4^{2-}$  intercalated LDHs.<sup>[44, 45]</sup> However, at 10 ppm of the M<sup>n+</sup> solutions, the (003) Bragg peak shifts from 1.08 to  $\sim 0.91$  nm which is equivalent to that of the LDH–NO<sub>3</sub>. It suggests that, at this concentration, the LDH–NO<sub>3</sub> regenerates by the exchange of  $Sn_2S_6$  anions. The nitrate anions are present in solution as the anion of the M<sup>n+</sup> salts used adsorption study. The presence of the (00*l*) peaks in the XRD diffraction patterns of the 100 ppm M<sup>n+</sup> adsorbed samples shows that they keep the nitrate intercalated LDH structure (Figure S4). SEM images confirm the retention of the hexagonal morphology of the crystallites at these concentrations. XRD patterns of the M<sup>n+</sup> adsorbed samples at concentrations  $\geq 1000$  ppm show the absence of the layered structures of LDH. This suggests that the LDH structure does not sustain at such extremely high metal concentrations.

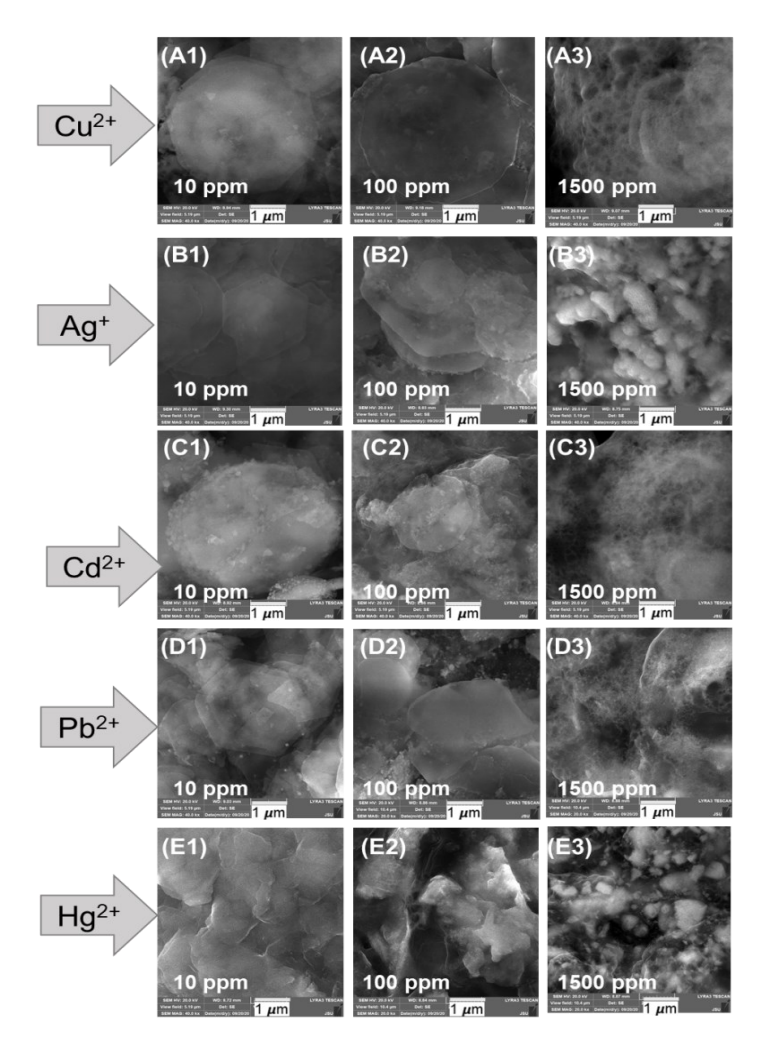


**Figure 6.** Scanning electron microscopy images of LDH–[Sn<sub>2</sub>S<sub>6</sub>], after the adsorption of 10, 100 and 1500 pm of Cu<sup>2+</sup> (A1, A2 and A3); Ag<sup>+</sup> (B1, B2, B3); Cd<sup>2+</sup> (C1, C2, C3); Pb<sup>2+</sup> (D1, D2, D3), and Hg<sup>2+</sup> (E1, E2, E3) demonstrating change in the morphology with the concentrations of heavy metal ions.

X-ray photoelectron spectroscopy (XPS) was conducted to determine the surface compositions and the chemical states of the post-adsorbed samples from 100 ppm solutions of  $Cu^{2+}$ ,  $Ag^+$ ,  $Cd^{2+}$ ,  $Pb^{2+}$ , and  $Hg^{2+}$  (Figure 7). XPS of the  $Cu^{2+}$ ,  $Ag^+$ ,  $Cd^{2+}$ ,  $Pb^{2+}$ , and  $Hg^{2+}$  adsorbed samples show the presence of these metals. For the  $Cu^{2+}$  adsorbed sample (Figure 7C), the bands centered at 932.3 and 952.5 eV correspond to the Cu 2p energy of the LDH–[ $Sn_2S_6$ ]. For the  $Ag^+$  adsorbed sample, two bands centered at 368.2 and 374.11 eV can

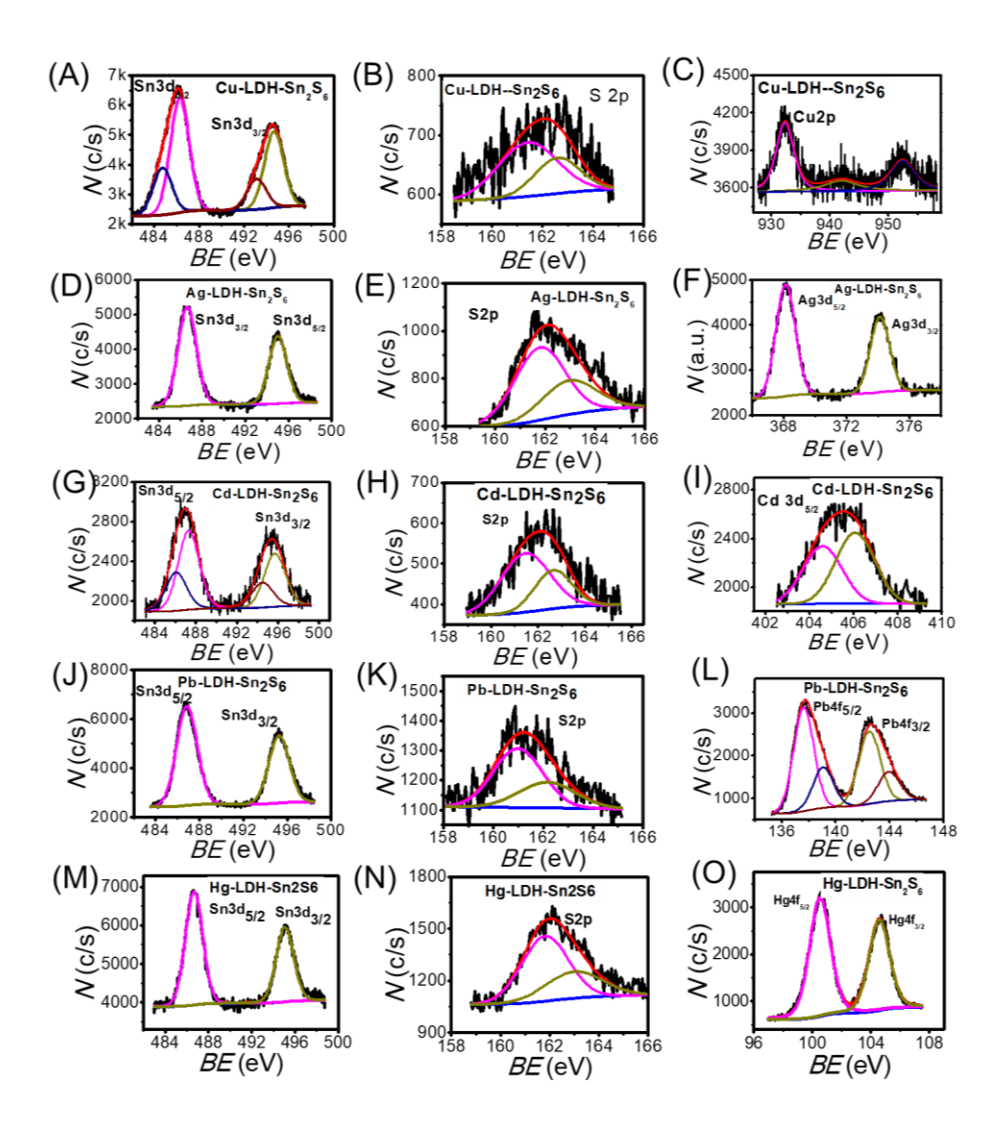


**Figure 7.** X-ray photoelectron spectra of LDH–[Sn<sub>2</sub>S<sub>6</sub>] after the adsorption of 100 ppm Cu<sup>2+</sup> (A-C); Ag<sup>+</sup> (D-F); Cd<sup>2+</sup> (G-I); Pb<sup>2+</sup> (J-L); and Hg<sup>2+</sup> (M-O).

be assigned to Ag 3d<sup>5/2</sup> and 3d<sup>3/2</sup> respectively.<sup>[79]</sup> The bands centered at 404.6 and 406.1 eV correspond to Cd 3d<sup>5/2</sup>, and 3d<sup>3/2</sup> obtained from the Cd<sup>2+</sup> adsorbed sample.<sup>[35, 79]</sup> For the Pb<sup>2+</sup> adsorbed sample, deconvolution of the peaks shows bands centered at 137.67/139.10 and 142.50/143.95 eV, respectively. These peaks originate from the 4f<sup>7/2</sup> and 4f<sup>5/2</sup> binding energies of Pb<sup>2+</sup>.<sup>[55]</sup> The energies of 137.67 and 142.50 eV (4f<sup>7/2</sup> and 4f<sup>5/2</sup>) correspond to the Pb<sup>2+</sup> of PbS;<sup>[55]</sup> while energies of 139.10 and 143.95 eV may originate from the 4f<sup>7/2</sup> and 4f<sup>5/2</sup> of Pb<sup>2+</sup> with a

different chemical environment, probably in the vicinity of the oxides.<sup>[80]</sup> The Hg<sup>2+</sup>-adsorbed sample reveals binding energies at 100.51 and 104.60 eV, which can be assigned as Hg 4f<sup>7/2</sup> and 4f<sup>5/2</sup>, respectively.<sup>[79]</sup> All the post-adsorption samples revealed Sn 3d bands in the range of 483-495 eV.<sup>[79]</sup> Deconvolution of the Sn 3d bands of Cu and Cd adsorbed samples yielded two sets of energy bands at 484.76/493.21 and 486.29/494.67 eV for Cu and 486.12/494.46 and 487.26//495.71 eV for Cd. [55] For the Ag<sup>+</sup>, Pb<sup>2+</sup>, and Hg<sup>2+</sup> adsorbed samples, only one set of bands of Sn 3d  $(3d^{5/2}, 3d^{3/2})$  was observed. These bands are centered at 486.61/495.06, 486.88/495.2 and 486.65/495.07 eV for Ag<sup>+</sup>, Pb<sup>2+</sup>, and Hg<sup>2+</sup>, respectively. [55, 79] The deviation of the binding energy of Sn 3d can be attributed to the diverse chemical environment of Sn<sup>4+</sup> cations. Moreover, the deconvoluted spectra of S 2p of the post adsorptions samples exhibit the binding energies of 161.45 and 162.65 eV for Cu<sup>2+</sup>, 161.86 and 163.08 eV for Ag<sup>+</sup>, 161.52 and 162.70 eV for Cd<sup>2+</sup>, 161.01 and 162.23 eV for Pb<sup>2+</sup>, and 161.82 and 163.07 for Hg<sup>2+</sup> (Figure 7).<sup>[54, 55, 79]</sup> These values are shifted from the S 2p peaks of the pristine LDH-[Sn<sub>2</sub>S<sub>6</sub>] with the binding energies in the range of 158.16-161.54 eV. These suggest that there is a notable change in the electronic states possibly attributed to the partial oxidation of S<sup>2-</sup> and/ formation of metal-sulfides.<sup>[80]</sup>

# 3.6 Analysis of the adsorption mechanisms of M<sup>n+</sup> by LDH-[Sn<sub>2</sub>S<sub>6</sub>]

XRD patterns of the pristine and the adsorbed samples provide intrinsic information about the structural features of the adsorbents. The adsorption mechanisms were investigated with respect to extremely low ( $\sim 1.0 \times 10^2$  ppb), medium ( $\sim 1.0 \times 10^4$  ppb) and extremely high ( $\sim 1.0 \times 10^6$  ppb) concentrations as shown in the scheme 1. At an extremely low concentration of  $M^{n+}$ , LDH–[Sn<sub>2</sub>S<sub>6</sub>] retains its layered structure with a little expansion of the basal spacing. This indicates that the interlayered Sn<sub>2</sub>S<sub>6</sub><sup>4-</sup> anions trap the inferior  $M^{n+}$  cations forming anionic complexes which remain inside the LDH gallery. A similar phenomenon has been observed in LDH-MoS<sub>4</sub>. [45] With

the increase of the concentrations of  $M^{n^+}$  ( $\geq 10$  ppm), the  $[Sn_2S_6]^{4^-}$  would combine with the  $M^{n^+}$  with a probable formation of electroneutral amorphous  $\{M^{n^+}[Sn_2S_6]^{4^-}\}$  which moves out of the LDH gallery. Concomitantly,  $NO_3^-$  anions of the nitrate salt of the cations enter into the interlayers and thus the LDH-NO3 regenerates. At concentrations  $\geq 10$  ppm, the adsorption mechanism probably varies with the type of  $M^{n^+}$ . For example, 100 ppm adsorbed samples, XRD of  $Cu^{2^+}$  and  $Ag^+$  adsorbed samples show a single phase LDH-NO3, while for the  $Cd^{2^+}$ ,  $Pb^{2^+}$  and  $Hg^{2^+}$  adsorbed samples LDH-NO3 coexists with the respective sulfides and sulfates (Figure S4). At extremely high concentrations ( $\geq 1000$  ppm), the introduction of a large amount of metal ions destroys the layered structure of LDH. The  $M^{n^+}$  cations bind with the  $S^{2^-}$  decomposed from  $[Sn_2S_6]^{4^-}$  generating metal sulfides or sulfates, where the latter is formed by the oxidation of sulfides.

**4. Application potential studied using tap and river water:** To assess the effects of the high concentrations of the cations and anions as well as the feasibility of LDH–[Sn<sub>2</sub>S<sub>6</sub>] to use for wastewater treatment, we studied the heavy metal uptake kinetics, selectivity, and efficiencies for tap and Mississippi river water (Table 4, Figure 8).

To perform this experiment, we spiked the tap water with a mixture of  $Co^{2+}$ ,  $Ni^{2+}$ ,  $Cu^{2+}$ ,  $Zn^{2+}$ ,  $Ag^+$ ,  $Cd^{2+}$ ,  $Pb^{2+}$ , and  $Hg^{2+}$  (Table 4) each at a concentration of 1 ppm, (1000 ppb; 8000 ppb in total). This experiment revealed LDH–[ $Sn_2S_6$ ] as an extremely efficient adsorbent for the concurrent removal of  $Cu^{2+}$ ,  $Ag^+$ ,  $Pb^{2+}$ ,  $Cd^{2+}$ , and  $Hg^{2+}$ . More precisely, in tap water, LDH–[ $Sn_2S_6$ ] can remove over 99.5% of  $Ag^+$ ,  $Cd^{2+}$ ,  $Pb^{2+}$ , and  $Hg^{2+}$  in seconds. Such an extremely rapid removal of cytotoxic  $Ag^+$ ,  $Cd^{2+}$ ,  $Pb^{2+}$ , and  $Hg^{2+}$  led to final concentrations of each cation of  $\leq 5$  ppb in less than 1 min (Figure 8A, Table 4) satisfying the WHO defined limit for safe drinking water. In 5 min, the removal capacity was increased to 99.8% for  $Ag^+$ ,  $Cd^{2+}$ ,  $Pb^{2+}$ , and  $Hg^{2+}$  resulting in final concentration of each cations as low as  $\leq 2$  ppb with  $K_d$  values remaining in the range of  $\sim 10^5$  to  $10^7$  mL/g. Notably,

in comparison to  $Ag^+$ ,  $Cd^{2+}$ ,  $Pb^{2+}$ , and  $Hg^{2+}$ , the  $Cu^{2+}$  is less selective and it takes about 15 min to reduce its concentration down to 2 ppb. Hence, the selectivity order that we determined in tap water is  $Zn^{2+}$ ,  $Co^{2+}$ ,  $Ni^{2+} << Cu^{2+} < Hg^{2+}$ ,  $Cd^{2+} < Pb^{2+}$ ,  $Ag^+$  which suggests that this material is extremely selective for the toxic  $Ag^+$ ,  $Cd^{2+}$ ,  $Pb^{2+}$ , and  $Hg^{2+}$  in tap water at ambient conditions and sorbes them within minutes.

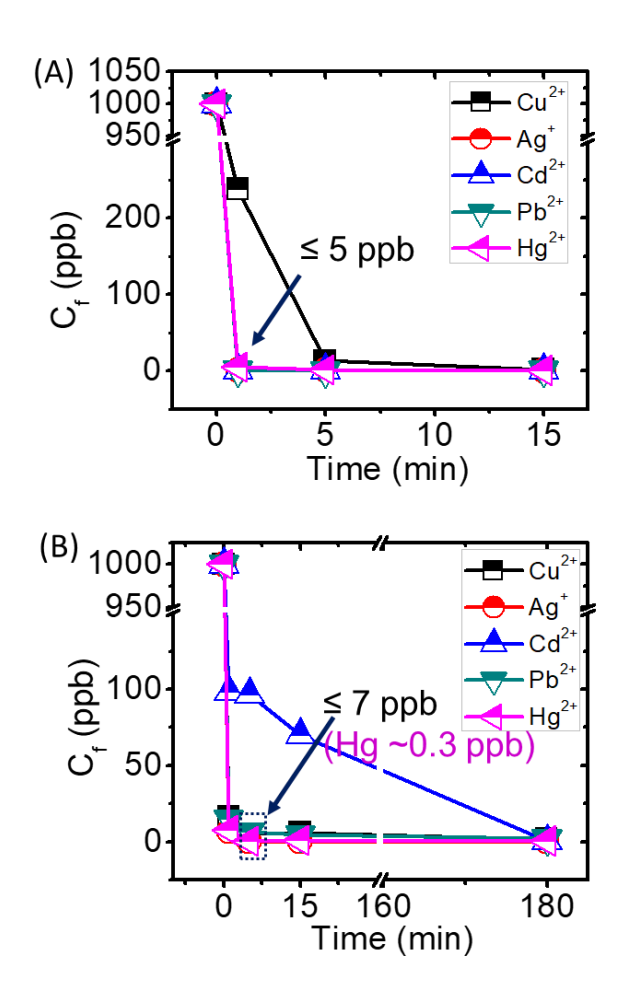


**Figure 8.** Concurrent adsorption kinetics curves of Cu<sup>2+</sup>, Ag<sup>+</sup>, Cd<sup>2+</sup>, Pb<sup>2+</sup>, and Hg<sup>2+</sup> obtained in tap water (A) and Mississippi river water (B) showing the highly efficient and rapid removal of the toxic cations from ppm to ppb levels.

Moreover, we studied the Mississippi river water (collected from Vidalia, Louisiana) and found that despite the presence of major background ions of Ca<sup>2+</sup>, Mg<sup>2+</sup>, Na<sup>+</sup>, Cl<sup>-</sup>, CO<sub>3</sub><sup>2-</sup>, SO<sub>4</sub><sup>2-</sup>, NO<sub>3</sub><sup>-</sup> and others, as well as a variety of organic species, LDH-[Sn<sub>2</sub>S<sub>6</sub>] shows an unprecedented sequestration of the  $Cu^{2+}$ ,  $Ag^+$ ,  $Cd^{2+}$ ,  $Pb^{2+}$ , and  $Hg^{2+}$ . In mixed-ion states of  $Co^{2+}$ ,  $Ni^{2+}$ ,  $Cu^{2+}$ ,  $Zn^{2+}$ ,  $Ag^+$ ,  $Cd^{2+}$ ,  $Pb^{2+}$ , and  $Hg^{2+}$  at concentrations of 1000 ppb for each (8000 ppb in total),  $LDH-[Sn_2S_6]$  stands out as extraordinary adsorbent for the simultaneous capture of Cu<sup>2+</sup>, Ag<sup>+</sup>, Pb<sup>2+</sup>, and Hg<sup>2+</sup> from ppm to ppb level just in 5 min satisfying the safe drinking water limit defined by US EPA and WHO (Table 4, Figure 9B). In contrast, the adsorption kinetics of Cd<sup>2+</sup> is relatively slow and after 3 h of interactions at mixed-states the residual concentrations of cadmium ion reach below one ppb. Our study shows that the selectivity order for the heavy metal cations of Zn<sup>2+</sup>, Co<sup>2+</sup>, Ni<sup>2+</sup>, Cu<sup>2+</sup>, Hg<sup>2+</sup>,  $Cd^{2+}$ ,  $Pb^{2+}$ ,  $Ag^{+}$  for the tap water spiked solutions is  $Zn^{2+}$ ,  $Co^{2+}$ ,  $Ni^{2+} << Cu^{2+} < Hg^{2+}$ ,  $Cd^{2+} < Pb^{2+}$ ,  $Ag^+$  while for the Mississippi river water it is  $Zn^{2+}$ ,  $Co^{2+}$ ,  $Ni^{2+} << Cd^{2+} < Cu^{2+}$ ,  $Hg^{2+} < Pb^{2+}$ ,  $Ag^+$ . In both experiments, LDH-[Sn<sub>2</sub>S<sub>6</sub>] efficiently and concurrently sequestered Cu<sup>2+</sup>, Ag<sup>+</sup>, Cd<sup>2+</sup>, Pb<sup>2+</sup>, and Hg<sup>2+</sup> from the waters. However, the sorption kinetics were relatively slow for the river water suggesting that the presence of highly concentrated numerous cations, anions, and organic species can affect the adsorption of heavy metals ions. Overall, LDH-[Sn<sub>2</sub>S<sub>6</sub>] is an unprecedented adsorbent that exhibits rapid, efficient, and the concurrent removal of  $Ag^+$ ,  $Cu^{2+}$ ,  $Pb^{2+}$ , and  $Hg^{2+}$ in the highly competitive ionic states of contaminated water of natural sources. Thus, this material can be used for the removal of Cu2+, Ag+, Cd2+, Pb2+, and Hg2+at trace level during the water purification process.

**Table 4.** Adsorption results of LDH– $[Sn_2S_6]$  toward mixed eight ions of 1 ppm for each (8 ppm total) in potable water and Mississippi river water,  $C_i$ = initial (pre-adsorption) concentration,  $C_f$  = final (post adsorption) concentration.

Mixed- ions	Time (min)	C <sub>i</sub> (ppm)	C <sub>f</sub>	Removal (%)	$K_d$ (mL/ $\alpha$ )	C <sub>f</sub> (ppm)	Removal (%)	$K_d$ (mL/g)
10115	(111111)	(ppiii)	(ppm) (%) (mL/g) <b>Tap water</b>			sissippi river water		
Co <sup>2+</sup>	<1	1.0	0.8080	19.13	$2.4 \times 10^{2}$	0.9979	0.21	2.10
	5	1.0	0.6880	31.17	$4.5 \times 10^2$	0.9501	4.99	$5.3 \times 10^{1}$
		1.0	0.0000	31.17	1.5 10	0.5501	1.,,,	2.5 10
Ni <sup>2+</sup>	<1	1.0	0.9990	0.06	6.0×10 <sup>-1</sup>	0.9573	4.27	$4.5 \times 10^{1}$
	5	1.0	0.9150	8.51	$9.3 \times 10^{1}$	0.8961	10.39	$1.2 \times 10^{2}$
$Zn^{2+}$	<1	1.0	0.9990	0.002	2.0×10 <sup>-2</sup>	0.9913	0.87	8.8
	5	1.0	0.8650	13.48	$1.5 \times 10^{2}$	0.9902	0.98	9.9
						j		
Cu <sup>2+</sup>	<1	1.0	0.2380	76.21	$3.2 \times 10^{3}$	0.0163	98.37	$6.0 \times 10^4$
	5	1.0	0.0130	98.74	$7.8 \times 10^4$	0.0050	99.50	$2.0 \times 10^{5}$
	15	1.0	0.0020	99.77	$4.4 \times 10^5$	0.0062	99.38	$1.6 \times 10^5$
$Ag^+$	<1	1.0	0.0001	99.99	$1.0 \times 10^7$	0.0070	99.30	$1.4 \times 10^{5}$
	5	1.0	0.0001	99.99	$1.0 \times 10^7$	0.0003	99.97	$3.3 \times 10^{6}$
	15	1.0	0.0001	99.99	$1.0 \times 10^7$	0.0001	99.99	$1.0 \times 10^{7}$
$Cd^{2+}$	<1	1.0	0.0040	99.62	$2.6 \times 10^5$	0.0985	90.15	$9.2 \times 10^{3}$
	5	1.0	0.0020	99.80	$5.0 \times 10^5$	0.0967	90.33	$9.3 \times 10^{3}$
	15	1.0	0.0001	99.99	$1.0 \times 10^7$	0.0700	93.00	$1.3 \times 10^4$
	180	-	-	-	-	0.0003	99.97	$3.3 \times 10^{6}$
Pb <sup>2+</sup>	<1	1.0	0.0001	99.99	$1.0 \times 10^7$	0.0147	98.53	$6.7 \times 10^4$
	5	1.0	0.0001	99.99	$1.0 \times 10^7$	0.0066	99.34	$1.5 \times 10^5$
	15	1.0	0.0001	99.99	$1.0 \times 10^7$	0.0045	99.55	2.2×10 <sup>5</sup>
	180	-	-	-	-	0.0002	99.98	$5.0 \times 10^6$
2.								-
$Hg^{2+}$	<1	1.0	0.0049	99.51	$2.0 \times 10^{5}$	0.0078	99.22	$1.3 \times 10^5$
	5	1.0	0.0012	99.87	$7.9 \times 10^5$	0.0003	99.97	$3.3 \times 10^6$
	15	1.0	0.0008	99.92	$1.2 \times 10^7$	0.0005	99.95	$2.0 \times 10^6$

(LDH-[Sn<sub>2</sub>S<sub>6</sub>]  $\sim 0.01$  g, volume of tap water 10 mL, v/m = 1000 mL/g and pH  $\sim \! 7)$ 

To evaluate regeneration and reusability, LDH-Sn<sub>2</sub>S<sub>6</sub> was investigated for the adsorption of the mixture of the solutions of  $Cu^{2+}$ ,  $Ag^+$ ,  $Cd^{2+}$ ,  $Pb^{2+}$ , and  $Hg^{2+}$  in five consecutive cycles (Figure 9, Table S10). These experiments were conducted using the total initial concentrations of 50 ppm of the mixed cations of  $Cu^{2+}$ ,  $Ag^+$ ,  $Cd^{2+}$ ,  $Pb^{2+}$ , and  $Hg^{2+}$  with 10 ppm of each element for each

cycle. Regeneration experiments were conducted using the 0.2 M EDTA as a complexing agent for heavy metals solutions after each cycle as described previously for Fe-MoS<sub>4</sub>. [68] The recycling experiments show that LDH-Sn<sub>2</sub>S<sub>6</sub> can efficiently remove Cu<sup>2+</sup>, Ag<sup>+</sup>, Cd<sup>2+</sup>, Pb<sup>2+</sup>, and Hg<sup>2+</sup> for a number of consecutive cycles. Notably, from the first through 5<sup>th</sup> cycles, LDH-Sn<sub>2</sub>S<sub>6</sub> removed over 99.9% of Ag<sup>+</sup> and Hg<sup>2+</sup> with  $K_d$  values of ~10<sup>6</sup> mL/g. In contrast, during the 5<sup>th</sup> cycle, LDH-Sn<sub>2</sub>S<sub>6</sub> removed about 97.8% of Cu<sup>2+</sup>, 96.7% of Cd<sup>2+</sup>, and 90.3% of Pb<sup>2+</sup> ions. A similar efficiency was also obtained for Ag<sup>+</sup> sorption by Fe-MoS<sub>4</sub>. [68] These consecutive reuse experiments show that LDH-Sn<sub>2</sub>S<sub>6</sub> remains efficient for the removal of Cu<sup>2+</sup>, Ag<sup>+</sup>, Cd<sup>2+</sup>, Pb<sup>2+</sup>, and Hg<sup>2+</sup> even after five consecutive cycles.

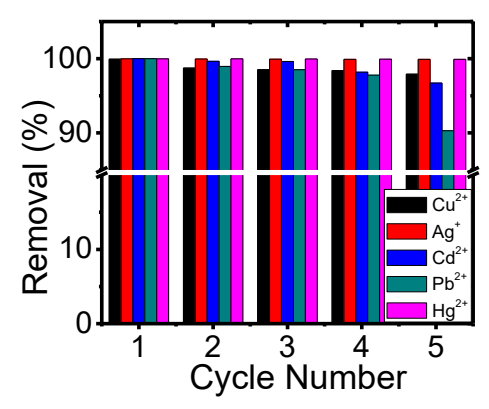


**Figure 9:** Recycling and separation of the heavy metals from a mixture of Cu<sup>2+</sup>, Ag<sup>+</sup>, Cd<sup>2+</sup>, Pb<sup>2+</sup>, and Hg<sup>2+</sup> from aqueous solutions in five consecutive cycles.

To determine the leaching of Mg<sup>2+</sup>, Al<sup>3+</sup> and Sn<sup>4+</sup> from the solid sorbent to the solutions during the adsorption of heavy metal ions, we analyzed the solutions after the sorption experiments of mixed solutions of Cu<sup>2+</sup>, Ag<sup>+</sup>, Pb<sup>2+</sup>, Cd<sup>2+</sup> and Hg<sup>2+</sup> (Table S11). Leaching of Sn<sup>4+</sup> resulted in a final solution concentration of 0.003 ppm which is equivalent to about 0.02% of total Sn in the sorbent. Greater solution concentrations were observed for Mg<sup>2+</sup> (23.3 ppm) and Al<sup>3+</sup> (9.7 ppm) corresponding to about 16 and 11%, respectively, of their total amounts in the solid matrix of LDH-Sn<sub>2</sub>S<sub>6</sub>. XRD of the solid sorbent after the adsorption shows the retention of LDH structure

which may demonstrate the topotactic exchange of the non-hazardous  $Mg^{2+}$  and  $Al^{3+}$  by heavy metal cations.

## 5. Conclusions

This study revealed the intercalation of the thiostannate anion, [Sn<sub>2</sub>S<sub>6</sub>]<sup>4</sup>, into the interlayer space of the solid-state matrix of LDHs using the chemistry of ion-exchange at ambient conditions. The soft polarizable Lewis basic characteristics of the sulfides (S2-) of the thiostannate anions of this novel hybrid LDH-[Sn<sub>2</sub>S<sub>6</sub>] exhibit tremendously high sorption and unprecedented selectivity for a wide number of Lewis acidic heavy metal cations. This material achieved over 99.9% concurrent uptake of Cu<sup>2+</sup>, Ag<sup>+</sup>, Cd<sup>+2</sup>, Pb<sup>2+</sup>, and Hg<sup>2+</sup> from the mixed-ions state of DIW, tap water, and river water maintaining  $K_d$  values over  $10^6$  mL/g. Strikingly, even in the presence of a large variety of competitive ions in the river water, LDH-Sn<sub>2</sub>S<sub>6</sub> simultaneously removed the cytotoxic Cu<sup>2+</sup>, Ag<sup>+</sup>, Pb<sup>2+</sup>, and Hg <sup>2+</sup> down to the WHO defined limit for drinking water in only 5 min. Moreover, LDH-Sn<sub>2</sub>S<sub>6</sub> can adsorb Cu<sup>2+</sup>, Ag<sup>+</sup>, Cd<sup>2+</sup>, Pb <sup>2+</sup>, and Hg <sup>2+</sup> with maximum sorption capacities of 378, 978, 332, 579, and 666 mg/g, respectively. Our study also revealed that LDH-[Sn<sub>2</sub>S<sub>6</sub>] is remarkably effective in acidic and basic solutions, capturing of over 99% of Cu<sup>2+</sup>, Ag<sup>+</sup>,  $Cd^{2+}$ ,  $Pb^{2+}$ , and  $Hg^{2+}$  with  $K_d$  values of  $> 10^5$  mL/g. The adsorption phenomena for  $Cu^{2+}$ ,  $Ag^+$ , Cd<sup>2+</sup>, Pb<sup>2+</sup>, and Hg<sup>2+</sup> can be demonstrated by the pseudo-second-order models which indicate a chemisorption process via metal sulfide bonds is involved the adsorption of M<sup>n+</sup> cations. The metal ion adsorption mechanism mainly includes the formation of interlayered [M<sup>n+</sup>Sn<sub>2</sub>S<sub>6</sub><sup>4-</sup>] complex and neutral metal-sulfides and depends on the M<sup>n+</sup>: LDH-Sn<sub>2</sub>S<sub>6</sub><sup>4-</sup> ratio. LDH-Sn<sub>2</sub>S<sub>6</sub> is recycable and can effeciently remove toxic heav metal cations to ppb levels over at least five consecutive cycles. Overall, our results suggest that LDH-[Sn<sub>2</sub>S<sub>6</sub>] is an unprecedented adsorbent that exhibits ultra-high heavy metal removal efficiencies, uptake kinetics, sorption capacity, robust selectivity,

and stability for a wide range of pHs. These fascinating findings place this cost-effective LDH-

[Sn<sub>2</sub>S<sub>6</sub>] at the top of any adsorbents known to date, and thus could be used for the decontamination

of heavy metal polluted wastewater.

ACKNOWLEDGEMENT: This work is partially supported by US Department of Energy

Environmental Management grant (MSIPP FY 2019 - RFP 0000458357) and NSF Division of

Chemistry (NSF-2100797). AC is thankful to Turkish Republic Ministry of National Education

for the partial support of his graduate studies stipend.

Any use of trade, firm, or product names is for descriptive purposes only and does not imply

endorsement by the U.S. Government.

Appendix A. and Supplementary data: Supplementary data of this article can be found online

at xxx

Author contributions: This manuscript was written through the contributions of all authors. All

authors have given approval to the final version of the manuscript.

**Notes**: The authors declare no financial interest

**AUTHOR INFORMATION** 

Corresponding Author:

muhammad.s.islam@jsums.edu

Department of Chemistry, Physics and Atmospheric Sciences

Jackson State University

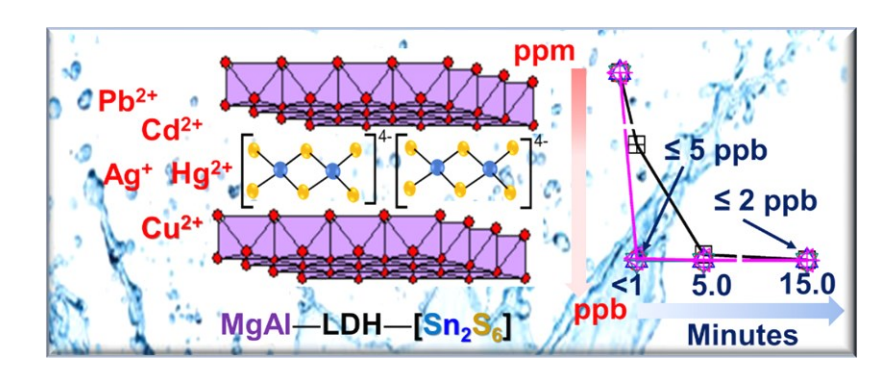
1400 J. R. Lynch Street

34

Jackson, MS 39217

NOTES: The authors declare no competing financial interest

**TOC Graphic**: LDH–[Sn<sub>2</sub>S<sub>6</sub>] is a unique adsorbent that combines an ultrahigh removal, superior selectivity, extremely rapid adsorption kinetics, a wide range of pH stability, and enormous adsorption capacity. The combinations of such extraordinary adsorption features place LDH-Sn<sub>2</sub>S<sub>6</sub> at the top of all materials known to date. Thus, this material could be used for the decontaminations of wastewater.



#### References

- [1] M. A. Shannon, P. W. Bohn, M. Elimelech, J. G. Georgiadis, B. J. Marinas, A. M. Mayes, Science and technology for water purification in the coming decades: A review. Nature, 452 (2008), 301-310.
- [2] W. A. Jury, H., Jr. Vaux, The role of science in solving the world's emerging water problems. Proc. Natl. Acad. Sci. 102 (2005), 15715-15720.
- [3] M. M. Mekonnen, A. Y. Hoekstra, Four billion people facing severe water scarcity. Sci. Adv. 2 (2016), e1500323.
- [4] P. H. Gleick, Global freshwater resources: soft-path solutions for the 21st century. Science 302 (2003), 1524-1528.
- [5] P. B. Tchounwou, C. G. Yedjou, A. K. Patlolla, D. J. Sutton, Heavy metal toxicity and the environment. Exp. Suppl. 101(2012), 133-164.
- [6] L. Joseph, B. M. Jun, J. R. V. Flora, C. M. Park, Y. Yoon, Removal of heavy metals from water sources in the developing world using low-cost materials: A review. Chemosphere, 229(2019), 142-159.
- [7] K. H. Vardhan, P. S. Kumar, R. C. Panda, A review on heavy metal pollution, toxicity and remedial measures: Current trends and future perspectives. J. Mol. Liq. 290(2019), 111197
- [8] X. Wu, S. J. Cobbina, G. Mao, H. Xu, Z. Zhang, L. Yang, A review of toxicity and mechanisms of individual and mixtures of heavy metals in the environment. Environ. Sci .Pollut. Res. Int. 23 (2016), 8244-8259.
- [9] N. Alia, K. Sardar, M. Said, K. Salma, A. Sadia, S. Sadaf, A. Toqeer, S. Miklas, Toxicity and bioaccumulation of heavy metals in spinach (spinacia oleracea) grown in a controlled environment, Int. J. Environ. Res. Public. Health 12 (2015), 7400-7416.
- [10] M. J. Manos, M. G. Kanatzidis, Layered metal sulfides capture uranium from seawater. J. Am. Chem. Soc. 134 (2012), 16441-16446.
- [11] J. Xu, C. Liu, P. C. Hsu, J. Zhao, T. Wu, J. Tang, K. Liu, Y. Cui, Remediation of heavy metal contaminated soil by asymmetrical alternating current electrochemistry. Nat. Commun. 10 (2019), 1-8.
- [12] R. Vidu, E. Matei, A. M. Predescu, B. Alhalaili, C. Pantilimon, C. Tarcea, C. Predescu, Removal of heavy metals from wastewaters: A challenge from current treatment methods to nanotechnology applications, Toxics, 8 (2020), 101
- [13] Y. Zhang, X. Duan, Chemical precipitation of heavy metals from wastewater by using the synthetical magnesium hydroxy carbonate. Water Sci. Technol. 81 (2020), 1130-1136.
- [14] M. M. Matlock, B. S. Howerton, D. A. Atwood, Chemical precipitation of heavy metals from acid mine drainage. Water. Res. 36 (2002), 4757-4764.
- [15] A. Ozverdi, M. Erdem, Cu<sup>2+</sup>, Cd<sup>2+</sup> and Pb<sup>2+</sup> adsorption from aqueous solutions by pyrite and synthetic iron sulfide. J. Hazard. Mater. 137 (2006), 626-632.
- [16] C. J. Rhodes, Properties and applications of zeolites. Sci. Prog. 93(2010), 223-284.
- [17] M. Elkady, H. Shokry, H. Hamad, New activated carbon from mine coal for adsorption of dye in simulated water or multiple heavy metals in real wastewater. Materials, 13 (2020), 2498
- [18] A. M. James, S. Harding, T. Robshaw, N. Bramall, M. D. Ogden, R. Dawso, Selective environmental remediation of strontium and cesium using sulfonated hyper-cross-linked polymers (SHCPs). ACS Appl. Mater. Interfaces 11(2019), 22464-22473.

- [19] S. Sarode, P. Upadhyay, M. A. Khosa, T. Mak, A. Shakir, S. Song, A. Ullah, Overview of wastewater treatment methods with special focus on biopolymer chitin-chitosan. Int. J. Biol. Macromol. 121(2019), 1086-1100.
- [20] J. P. Bezzina, L. R. Ruder, R. Dawson, M. D. Ogden, Ion exchange removal of Cu(II), Fe(II), Pb(II) and Zn(II) from acid extracted sewage sludge Resin screening in weak acid media. Water Res. 158(2019), 257-267.
- [21] M. G. da Fonseca, M. M. de Oliveira, L. N. Arakaki, Removal of cadmium, zinc, manganese and chromium cations from aqueous solution by a clay mineral. J. Hazard. Mater. 137 (2006), 288-292.
- [22] M. J. Manos, M. G. Kanatzidis, Sequestration of heavy metals from water with layered metal sulfides. Chemistry, 15 (2009), 4779-4784.
- [23] X. H. Qi, K. Z. Du, M. L. Feng, Y. J. Gao, X. Y. Huang, M. G. Kanatzidis, Layered A<sub>2</sub>Sn<sub>3</sub>S<sub>7</sub>.1.25H<sub>2</sub>O (A = organic cation) as efficient ion-exchanger for rare earth element recovery.J. Am. Chem. Soc. 139 (2017), 4314-4317.
- [24] R. G. Pearson, Hard and soft acids and bases. J. Am. Chem. Soc. 85(1963), 3533-3539.
- [25] R. G. Parr, R. G. Pearson, Absolute hardness: companion parameter to absolute electronegativity. J. Am. Chem. Soc. 105(1983), 7512-7516.
- [26] M. L. Feng, D. Sarma, X. H. Qi, K. Z. Du, X. Y. Huang, M. G. Kanatzidis, Efficient removal and recovery of uranium by a layered organic-inorganic hybrid thiostannate. J. Am. Chem. Soc. 138 (2016), 12578-12585.
- [27] M. J. Manos, K. Chrissafis, M. G. Kanatzidis, Unique pore selectivity for  $Cs^+$  and exceptionally high  $NH_4^+$  exchange capacity of the chalcogenide material  $K_6Sn[Zn_4Sn_4S_{17}]$ . J. Am. Chem. Soc.128 (2006), 8875-8883.
- [28] L. Mercier, T. J. Pinnavaia, Access in mesoporous materials: Advantages of a uniform pore structure in the design of a heavy metal ion adsorbent for environmental remediation. Adv. Mater. 9(1997), 500-503.
- [29] M. J. Manos, N. Ding, M. G. Kanatzidis, Layered metal sulfides: exceptionally selective agents for radioactive strontium removal. Proc. Natl. Acad. Sci. 105 (2008), 3696-3699.
- [30] M. J. Manos, C. D. Malliakas, M. G. Kanatzidis, Heavy-metal-ion capture, ion-exchange, and exceptional acid stability of the open-framework chalcogenide (NH<sub>4</sub>)<sub>4</sub>In<sub>12</sub>Se<sub>20</sub>. Chemistry, 13 (2007), 51-58.
- [31] M. J. Manos, M. G. Kanatzidis, Highly efficient and rapid Cs<sup>+</sup> uptake by the layered metal sulfide K<sub>2x</sub>Mn<sub>x</sub>Sn<sub>3-x</sub>S<sub>6</sub> (KMS-1). J. Am. Chem. Soc. 131 (2009), 6599-65607.
- [32] M. J. Manos, V. G. Petkov, M. G. Kanatzidis,  $H_{2x}Mn_xSn_{3-x}S_6$  (x = 0.11–0.25): A novel reusable sorbent for highly specific mercury capture under extreme pH conditions. Adv. Funct. Mater.19 (2009), 1087-1092.
- [33] Z. H. Fard, C. D. Malliakas, J. L. Mertz, M. G. Kanatzidis, Direct extraction of  $Ag^+$  and  $Hg^{2+}$  from cyanide complexes and mode of binding by the layered  $K_2MgSn_2S_6$  (KMS-2). Chem. Mater. 27 ( 2015), 1925–1928.
- [34] J. L. Mertz, Z. H. Fard, C. D. Malliakas, M. J. Manos, M. G. Kanazidis, Selective removal of  $Cs^+$ ,  $Sr^{2+}$ , and  $Ni^{2+}$  by  $K_{2-x}$   $Mg_x$   $Sn_{3-x}S_6$  (x=0.5-1)(KMS-2) Relevant to Nuclear Waste remediation. Chem. Mater. 25 (2013), 2116-2127.
- [35] D. Sarma, C. D. Malliakas, K. S. Subrahmanyam, S. M. Islam, M. G. Kanatzidis,  $K_{2x}$  Sn<sub>4-x</sub> S<sub>8-x</sub> (x = 0.65-1): a new metal sulfide for rapid and selective removal of Cs<sup>+</sup>, Sr<sup>2+</sup> and UO<sub>2</sub><sup>2+</sup> ions. Chem. Sci. 7 (2016), 1121-1132.

- [36] M. L. Feng, D. N. Kong, Z. L. Xie, X. Y. Huang, Three-dimensional chiral microporous germanium antimony sulfide with ion-exchange properties. Angew, Chem, Int. Ed. Engl. 47 (2008), 8623-8626.
- [37] Z. H. Fard, S. M. Islam, M. G. Kanatzidis, Porous amorphous chalcogenides as selective adsorbents for heavy metals. Chem. Mater. 27(2015), 6189–6192.
- [38] Y. Oh, S. Bag, C. D. Malliakas, M. G. Kanatzidis, Selective surfaces: high-surface-area zinc tin sulfide chalcogels. Chem. Mater. 23(2011), 2447-2456.
- [39] M. Yuan, H. Yao, L. Xie, X. Liu, H. Wang, S. M. Islam, K. Shi, Z. Yu, G. Sun, H. Li, S.
- Ma, M. G. Kanatzidis, Polypyrrole-Mo<sub>3</sub>S<sub>13</sub>: An efficient sorbent for the capture of Hg<sup>2+</sup> and highly selective extraction of Ag<sup>+</sup> over Cu<sup>2+</sup>. J. Am. Chem. Soc. 142 (2020), 1574-1583.
- [40] L. Xie, Z. Yu, S. M. Islam, K. Shi, Y. Cheng, M. Yuan, J. Zhao, G. Sun, H. Li, S. Ma, M. G. Kanatzidis, Remarkable acid stability of polypyrrole-MoS<sub>4</sub>: ahighly selective and efficient scavenger of heavy metals over a wide pH range.Adv. Funct. Mater. 28 (2018), 1800502.
- [41] S. Ma, S. M. Islam, Y. Shim, Q. Gu, P. Wang, H. Li, G. Sun, X. Yang, M. G. Kanatzidis, Highly efficient iodine capture by layered double hydroxides intercalated with polysulfides. Chem. Mater. 26(2014), 7114–7123.
- [42] W. He, K. Ai, X. Ren, S. Wang, L. Lu, Inorganic layered ion-exchangers for decontamination of toxic metal ions in aquatic systems. J. Mater. Chem. A, 5(2017), 19593-19606.
- [43] S. Gu, X. Kang, L. Wang, E. Lichtfouse, C. Wang, Clay mineral adsorbents for heavy metal removal from wastewater: A review. Environ. Chem. Lett. 17(2019), 629–654
- [44]S. Ma. Q. Chen, H. Li, P. Wang, S. M. Islam, Q. Gu, X. Yang, M. G. Kanatzidis, Highly selective and efficient heavy metal capture with polysulfide intercalated layered double hydroxides. J. Mater. Chem. A, 2(2014), 10280-10289.
- [45] L. Ma, Q. Wang, S. M. Islam, Y. Liu, S. Ma, M. G. Kanatzidis, Highly selective and efficient removal of heavy metals by layered double hydroxide intercalated with the MoS<sub>4</sub><sup>2</sup>-ion. J. Am. Chem. Soc.138 (2016), 2858-2866.
- [46]S. Ma, C. Fan, L. Du, G. Huang, X. Yang, W. Tang, Y. Makita, K. Ooi, Intercalation of macrocyclic crown ether into well-crystallized LDH: formation of staging structure and secondary host—guest reaction. Chem. Mater. 21 (2009), 3602–3610.
- [47] S. Ma, J. Wang, L. Du, Y. Sun, Q. Gu, G. Sun, X. Yang, A new method for fast intercalation of bulk crown ether guest into LDH. J. Colloid. Interface. Sci. 393(2013), 29-35.
- [48] M. G. Kanatzidis, B. Riley, J. Chun, Novel metal sulfides to achieve effective capture and durable consolidation of radionuclides. United States, (2016), DOE/NEUP--12-343.
- [49] G. A. Marking, J. A. Hanko, M. G. Kanatzidis, New quaternary thiostannates and thiogermanates  $A_2Hg_3M_2S_8$  (A = Cs, Rb; M = Sn, Ge) through molten  $A_2Sx$ . reversible glass formation in  $Cs_2Hg_3M_2S_8$ . Chem. Mater.10 (1998), 1191–1199.
- [50] G. A. Marking, M. G. Kanatzidis, Encapsulation of cyclooctasulfur molecules in an open metal-sulfide framework. isolation of the host-guest complex Cs<sub>2</sub>Sn<sub>3</sub>S<sub>7</sub>·1/2S<sub>8</sub> from molten cesium polysulfide fluxes. Chem. Mater.7 (1995), 1915–1921.
- [51] L. P. F. Benício, D. Eulálio, L. d. M. Guimarães, F. G. Pinto, L. M. da Costa, J. Tronto, J. Layered double hydroxides as hosting matrices for storage and slow release of phosphate analyzed by stirred-flow method. Mater. Res. 21(2018), e20171004.
- [52] M. H. Brooker, Raman study of the structural properties of  $KNO_3(II)$ . Can. J. Chem. 55(1977), 1242-1250.

- [53] D. Cosano, D. Esquivel, F. J. Romero-Salguero, C. Jiménez-Sanchidrián, J. R. Ruiz, Use of raman spectroscopy to assess nitrate uptake by calcined LDH phases. Colloids Surf, A Physicochem. Eng. Asp. 602(2020), 125066.
- [54] S. M. Islam, C. D. Malliakas, D. Sarma, D. C. Maloney, C. C. Stoumpos, O. Y. Kontsevoi, A. J. Freeman, M. G. Kanatzidis, Direct gap semiconductors Pb<sub>2</sub>BiS<sub>2</sub>I<sub>3</sub>, Sn<sub>2</sub>BiS<sub>2</sub>I<sub>3</sub>, and Sn<sub>2</sub>BiSI<sub>5</sub>.Chem. Mater. 28(2016), 7332-7343.
- [55] J. F. Moulder, Handbook of X-Ray Photoelectron Spectroscopy: A reference book of standard spectra for identification and interpretation of XPS data. Perkin-Elmer Corporation, Physical Electronics Division: Eden Prairie, USA, 1995.
- [56] S. M. Islam, K. S. Subrahmanyam, C. D. Malliakas, M. G. Kanatzidis, One-dimensional molybdenum thiochlorides and their use in high surface area MoS<sub>x</sub>chalcogels. Chem. Mater. 26(2014), 5151-5160.
- [57] X. Y. Yu, T. Luo, Y. X. Zhang, Y. Jia, B. J. Zhu, X. C. Fu, J. H. Liu, X. J. Huang, Adsorption of lead(II) on O<sub>2</sub>-plasma-oxidized multiwalled carbon nanotubes: thermodynamics, kinetics, and desorption. ACS Appl. Mater. Interfaces, 3 (2011), 2585-2593.
- [58] Agency, U. S. E. P., 2018 edition of the drinking water standards and health advisories tables, https://www.epa.gov/sites/production/files/2018-03/documents/dwtable2018.pdf, Dec. 2013. Washington, DC, 2018(accessed 20 December 2020)
- [59]WHO, Guidelines for drinking-water quality, 4th edition, incorporating the 1st addendum. Organization, 2017.
- [60] D. Sarma, S. M. Islam, K. S. Subrahmanyam, M. G. Kanatzidis, Efficient and selective heavy metal sequestration from water by using layered sulfide  $K_{2x}Sn_{4-x}S_{8-x}$  (x = 0.65-1; KTS-3). J. Mater. Chem. A, 4(2016), 16597-16605.
- [61] T. Liu, M. Yang, T. Wang, Q. Yuan, Prediction strategy of adsorption equilibrium time based on equilibrium and kinetic results to isolate taxifolin.Ind. Eng. Chem. Res. 51(2012), 454–463.
- [62] S. Azizian, Kinetic models of sorption: a theoretical analysis. J. Colloid. Interface Sci. 276 (2004), 47-52.
- [63] A. K. Bhattacharya, T. K. Naiya, S. N. Mandal, S. K. Das, Adsorption, kinetics and equilibrium studies on removal of Cr(VI) from aqueous solutions using different low-cost adsorbents. Chem. Engineer. J.137(2008), 529-541.
- [64] S. Deng, Y. P. Ting, Polyethylenimine-modified fungal biomass as a high-capacity biosorbent for Cr(VI) anions: sorption capacity and uptake mechanisms. Environ. Sci. Technol. 39 (2005), 8490-8496.
- [65] T. S. Anirudhan, P. S. Suchithra, Synthesis and characterization of tannin-immobilized hydrotalcite as a potential adsorbent of heavy metal ions in effluent treatments. Appl. Clay Sci. 42(2008), 214-223.
- [66] M. A. González, I. Pavlovic, C. Barriga, Cu(II), Pb(II) and Cd(II) sorption on different layered double hydroxides. a kinetic and thermodynamic study and competing factors. Chem. Eng. J. 269(2015), 221–228.
- [67] X. Luo, X. Lei, N. Cai, X. J. Xie, Y. Xue, F. Yu, Removal of heavy metal ions from water by magnetic cellulose-based beads with embedded chemically modified magnetite nanoparticles and activated carbon. ACS Sustainable Chem. Eng. 4 (2016), 3960–3969.
- [68] A. Jawad, Z. Liao, Z. Zhou, A. Khan, T. Wang, J. Ifthikar, A. Shahzad, Z. Chen, Z. Chen, Fe-MoS<sub>4</sub>: An effective and stable LDH-based adsorbent for selective removal of heavy metals. ACS Appl. Mater. Interfaces. 9 (2017), 28451-28463.

- [69] J. J. Alcaraz-Espinoza, A. E. Chavez-Guajardo, J. C. Medina-Llamas, C. A. Andrade, C. P. de Melo, Hierarchical composite polyaniline-(electrospun polystyrene) fibers applied to heavy metal remediation. ACS Appl. Mater. Interfaces, 7(2015), 7231-7240.
- [70] J. R. Li, X. Wang, B. Yuan, M. L. Fu, Layered chalcogenide for Cu<sup>2+</sup> removal by ion-exchange from wastewater. J. Mol. Liq.200(2014), 205-212.
- [71] G. Rathee, S. Kohli, A. Awasthi, N. Singh, R. Chandra, MoS<sub>4</sub><sup>2-</sup> intercalated NiFeTiLDH as an efficient and selective adsorbent for elimination of heavy metals. RSC Adv. 10(2020), 19371-19381.
- [72] J. Ali, H. Wang, J. Ifthikar, A. Khan, T. Wang, K. Zhan, A. Shahzad, Z. Z. Chen, Chen, Efficient, stable and selective adsorption of heavy metals by thio-functionalized layered double hydroxide in diverse types of water. Chem. Eng. J. 332(2018), 387-397.
- [73] H. Asiabi, Y. Yamini, M. Shamsayei, E. Tahmasebi, Highly selective and efficient removal and extraction of heavy metals by layered double hydroxides intercalated with the diphenylamine-4-sulfonate: a comparative study. Chem. Eng. J. 323(2017), 212-223.
- [74] M. Zhang, Q. Yin, X. Ji, F. Wang, X. Gao, M. Zhao, High and fast adsorption of Cd(II) and Pb(II) ions from aqueous solutions by a waste biomass based hydrogel. Sci. Rep. 10 (2020), 1-13.
- [75] K. Wang, J. Gu, N. Yin, Efficient removal of Pb(II) and Cd(II) Using NH<sub>2</sub>-functionalized Zr-MOFs via rapid microwave-promoted synthesis. Ind. Eng. Chem. Res. 56 (2017), 1880–1887. [76] D. T. Sun, L. Peng, W. S. Reeder, S. M. Moosavi, D. Tiana, D. K. Britt, E. Oveisi, W. L.
- Queen, Rapid, selective heavy metal removal from water by a metal-organic framework/polydopamine composite. ACS Cent. Sci. 4 (2018), 349-356.
- [77] M. Ogawa, F. Saito, Easily oxidizable polysulfide anion occluded in the interlayer space of Mg/Al layered double hydroxide. Chem. Lett. 33 (2004), 1030-1031.
- [78] S. M. Alatalo, F. Pileidis, E. Makila, M. Sevilla, E. Repo, J. Salonen, M. Sillanpaa, M. M. Titirici, Versatile cellulose-based carbon aerogel for the removal of both cationic and anionic metal contaminants from water. ACS Appl. Mater. Interfaces, 7(2015), 25875-25883.
- [79] L. Ma, S. M. Islam, C. Xiao, J. Zhao, H. Liu, M. Yuan, G. Sun, H. Li, S. Ma, M. G. Kanatzidis, Rapid simultaneous removal of toxic anions [HSeO<sub>3</sub>]<sup>-</sup>, [SeO<sub>3</sub>]<sup>2</sup>-, and [SeO<sub>4</sub>]<sup>2</sup>-, and metals Hg<sup>2+</sup>, Cu<sup>2+</sup>, and Cd<sup>2+</sup> by MoS<sub>4</sub><sup>2-</sup>intercalated layered double hydroxide. J. Am. Chem. Soc.139 (2017), 12745-12757.
- [80] D. J. Cant, K. L. Syres, P. J. Lunt, H. Radtke, J. Treacy, P. J. Thomas, E. A. Lewis, S. J. Haigh, P. O'Brien, K. Schulte, F. Bondino, E. Magnano, W. R. Flavell, Surface properties of nanocrystalline PbS films deposited at the water-oil interface: a study of atmospheric aging. Langmuir, 31 (2015), 1445-1453.
- [81] K. Chondroudis, T. J. McCarthy, M. G. Kanatzidis, Chemistry in molten alkali metal polyselenophosphate fluxes. Influence of flux composition on dimensionality. Layers and chains in APbPSe<sub>4</sub>, A<sub>4</sub>Pb(PSe<sub>4</sub>)<sub>2</sub>(A= Rb, Cs), and K<sub>4</sub>Eu(PSe<sub>4</sub>)<sub>2</sub>. Inorg. Chem. 35(1996), 840-844.
- [82] M. G. Kanatzidis, T. J. McCarthy, T. A. Tanzer, L. H.Chen, L. Iordanidis, T. Hogan, C. R. Kannewurf, C. Uher, B. Chen, Synthesis and thermoelectric properties of the new ternary bismuth sulfides KBi<sub>6.33</sub>S<sub>10</sub> and K<sub>2</sub>Bi<sub>8</sub>S<sub>13</sub>.Chem. Mater.8(1996), 1465–1474.